Ore Geology Reviews 142 (2022) 104700

Contents lists available at ScienceDirect

Ore Geology Reviews

journal homepage: www.elsevier.com/locate/oregeorev

# Significant enrichment of Rb and Cs in the Late Triassic coals from the Coc Sau surface mine, Cam Pha Coalfield, Quang Ninh Province, Vietnam

Xuanphu Nguyen [a,b], Jing Li [a,*], Xinguo Zhuang [a], Baoqing Li [a], Xavier Querol [c], Natalia Moreno [c], Patricia Cordoba [c]

[a] Key Laboratory of Tectonics and Petroleum Resources (China University of Geosciences), Ministry of Education, Wuhan 430074, China
[b] Department of Prospecting and Exploration Geology, Hanoi University of Mining and Geology, Hanoi, Viet Nam
[c] Institute of Environmental Assessment and Water Research, IDÆA-CSIC C/Jordi Girona, 18-26, Barcelona 08034, Spain

ARTICLE INFO

*Keywords:*
Coal geochemistry
Minerals in coal
Rb and Cs enrichment in coal
Late Triassic coals
Cam Pha Coalfield

ABSTRACT

The current study investigates the mineralogical and geochemical characteristics of the Late Triassic coals from the Coc Sau open-pit mine, Cam Pha Coalfield (Quang Ninh Province, Northeastern Vietnam) using Powder X-ray diffraction (XRD), field emission-scanning electron microscopy (FE-SEM), inductively coupled plasma atomic-emission spectrometry (ICP-AES) and inductively coupled plasma mass spectrometry (ICP-MS). Coals from Coc Sau open-pit mine are characterized by medium ash yield (avg. 29.7%), low sulfur content (avg. 0.17%), and low moisture content (avg. 1.8%). The volatile matter content (avg. 8.4%) indicates a semianthracite rank. The crystalline phases identified in Coc Sau coals and host rocks (roof, floor, parting) are primarily quartz, kaolinite and muscovite, with small proportions of ankerite, clinochlore, anatase, calcite, and tobelite. Illite, pyrite, and siderite were occasionally detected in individual samples. In addition, several minerals below the XRD detection limit, such as barite, apatite, zircon, xenotime, and florencite were observed by SEM. The low sulfur concentrations, low Sr/Ba ratio and relatively high ash yield of these coals indicate a continental lake basin sedimentary environment with a relatively strong supply of terrigenous detritus. Quartz, kaolinite, and muscovite were most likely derived from the terrigenous source region surrounding the basin, and the other minerals are mainly of authigenic origin. Relative to worldwide coals, the Coc Sau coals and host rocks are highly enriched in Rb and Cs, which can be a potential source for Rb and Cs recovery during coal utilization and combustion. Rubidium and Cs enriched in the coals are positively correlated with Al and K, indicating that they most likely occur in potassium-rich clay minerals (e.g., muscovite), and originate from weathered felsic terrigenous detritus.

## 1. Introduction

The study about mineralogy and geochemistry of coal can provide some useful information for understanding the coal quality and paleo-environmental conditions, such as depositional conditions, climatic and hydrological conditions, provenance region, tectonic setting history and diagenetic and epigenetic process (Brownfield et al., 1995; Dai et al., 2012, 2020, 2021; Finkelman et al., 2019; Karayigit et al., 2020; Seredin and Finkelman, 2008; Swaine and Goodarzi, 1995; Ward, 2002). In addition, the concentrations, and modes of occurrence of hazardous trace elements in coals are potential detrimental factors for environmental pollution and effects on human health during coal combustion/utilization (Finkelman et al., 2002; Finkelman and Tian, 2017). For example, Querol et al (2008) investigated the coal gangue from Shanxi Province, China and reported that some potential hazardous elements (e.g., As, S, N, Hg, and Se) emitted during spontaneous coal gangue combustion may cause environmental problems. Dai et al (2012) studied the geochemistry of trace elements in Chinese coals and ascribed the high concentration of some toxic elements (As, F, and Se) released to the air during coal combustion as the main source of endemic diseases (endemic arsenosis, fluorosis, and selenosis).

On the other hand, coals can be regarded as a promising source for recovery of several critical elements (e.g., Ge, Ga, U, V, Se, rare earth elements and Y (REY or REE if Y is not included), Nb, etc.) and base metals (e.g., Al and Mg) (Dai et al., 2012, 2018, 2021; Dai and Finkelman, 2018; Seredin and Dai, 2012; among others). For instance, germanium has been extracted at industrial scale from coal combustion products for many years. It is estimated that over half of global industrial

* Corresponding author.
*E-mail address:* jingli@cug.edu.cn (J. Li).

https://doi.org/10.1016/j.oregeorev.2022.104700
Received 16 November 2021; Received in revised form 30 December 2021; Accepted 5 January 2022
Available online 10 January 2022

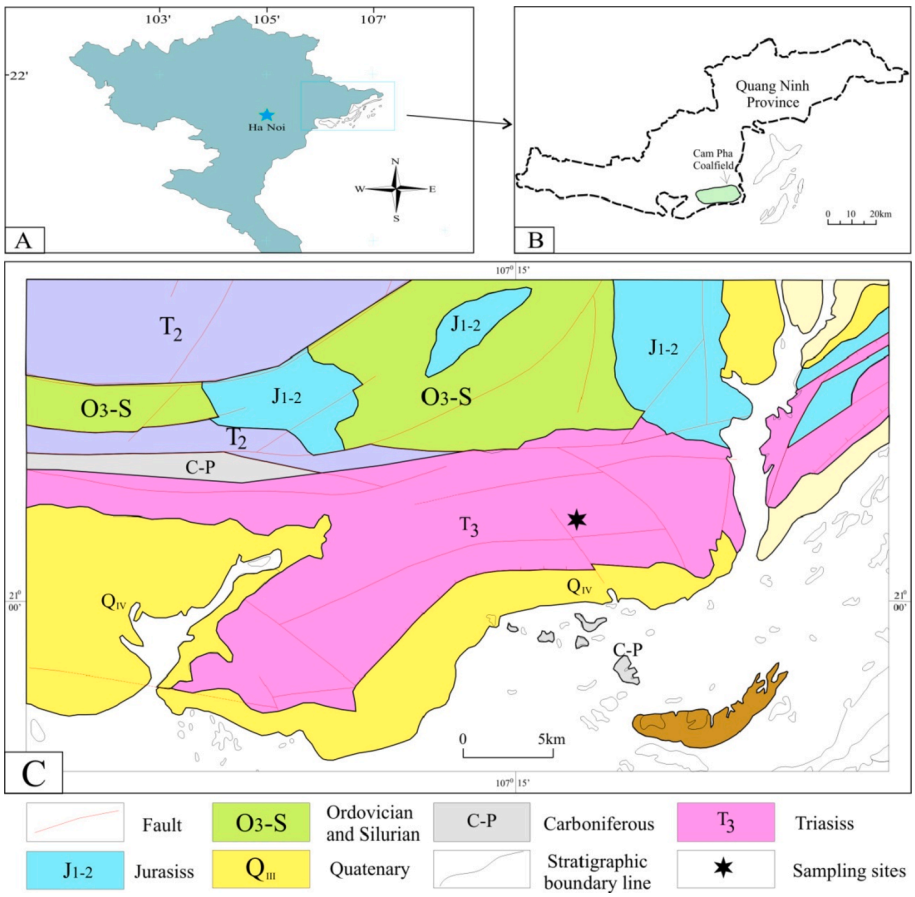


**Fig. 1.** Geological location of the studied area and sampling site. A; B: Overview map of Northern part of Vietnam and the location of Quang Ninh Province. C. The simplified geological map of Cam Pha coalfield (modified from Hung, 1997) and sampling sites.

Ge production are supplied by three coal-hosted high-Ge deposits (Lincang and Wulantuga, China; Spetzugli, Russian, Dai et al., 2014; Seredin and Finkelman, 2008). Uranium had been once industrially utilized just after world war II and has also been found significantly enriched in a number of coals (Seredin and Finkelman, 2008; Dai and Finkelman, 2018; Dai et al., 2015a, 2015b; Hower et al., 2016).

Vietnam is a country with great potential of coal reserves (about 55.59 billion tons in mainland) (Tri and Khuc, 2011), where coal has been explored and exploited for a long time and has made important contributions to the development of the national economy as well as large proportion of coal export. Located in the north-eastern part of Vietnam, Quang Ninh coal basin is one of the largest regions with significant potential for anthracite coal resource, accounting for 89% of total anthracite amount throughout Vietnam (Chinh et al., 2007). The coal management and exploitation in this region has been carried out by Vietnam national coal – mineral industries holding corporation limited (VINACOMIN) since 1995. According to VINACOMIN, the total anthracite coal reserves in this region are about 3.5 billion tons (in depth of −400 m), and the capacity from opencast mines and underground are approximately 35 million tons per year. In the 1960s and 1970s, several studies were carried out on coal and coal-bearing series in Quang Ninh coal basin, most of which has focused on identifying the basic coal quality, tectonic structural and stratigraphic evolution history (Luong, 1970; Quang, 1971; Tieu, 1971; Tri et al., 1977). The age of coal and coal-bearing strata, sedimentary facies, and coal rank have also been discussed (Hien and Binh, 1966a,b; Ich and Chi, 1972; Quang, 1969). Basic qualities of the Quang Ninh coals, such as moisture content, ash yield, volatile matter content, sulfur content, and calorific value, have been demonstrated by a few researches. Ash yield of the Quang Ninh basin coals generally ranges from 10 to 30%, and sulfur content from 0.5 to 0.7% (Hoang et al., 2001) with the exception that coals in Cam Pha, Hon Gai, Mao Khe, Trang Bach, and Vang Danh consist of quite high ash yield (31–39%, Baruya, 2010). Nonetheless, research on the mineralogy and geochemistry of coals in Quang Ninh coal region or even in the whole Vietnam has barely been conducted. Therefore, the knowledge about potential hazardous and critical elements in coals is scarce.

Given the issues discussed above, the present study aims at investigating the mineralogical and geochemical characteristics of coals from the Coc Sau surface mine, Cam Pha coalfield, Quang Ninh coal basin, with special emphasis on illustrating the enrichment, modes of occurrence and origin of potential elevated trace elements in coals from the Quang Ninh coal basin. This is the first comprehensive research on the enrichment of critical elements (Rb and Cs in the present study) in Vietnamese coals, which will provide significant theoretical guidance for the integrated and clean utilization of coal resources in Vietnam.

## 2. Geological setting

Tectonism during the Mesozoic formed many graben depressions which are filled with coal-bearing terrigenous sediments (e.g., Hon Gai Formation, Van Lang Formation, Suoi Bang Formation, Dong Do Formation) in northeast of Vietnam. These graben depressions were

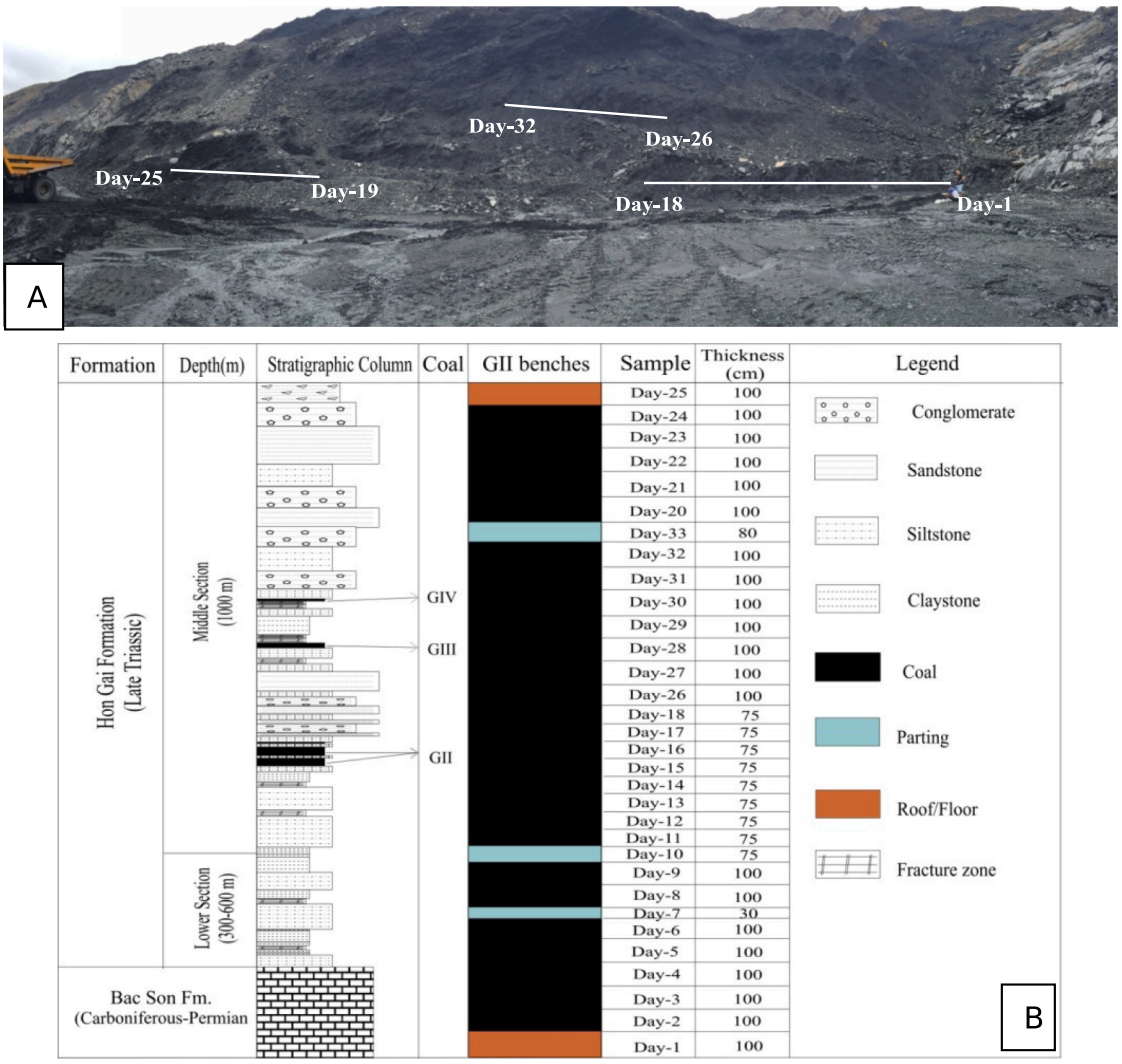


**Fig. 2.** Location of sampling sites and stratigraphic column of the Coc Sau surface mine, Cam Pha coalfield. A, Location of sampling sites; B, Stratigraphic column and location of coal benches.

primarily composed of conglomerate, sandstone, coaly clay and industrial coal seams, which have been deposited in complex sedimentary facies such as alluvial, proluvium, delta plain, lakes, swamps, and dramatically change in both horizontal and vertical direction (Binh, 2005). The coal formation stages may start from the late Triassic and last to the early Jurassic, but are mostly of the Triassic Norian-Rhaetian ($T_3$n-*rhg*) (Tri et al., 2000).

The Quang Ninh coal basin is a coal-bearing graben depression, which consists of two main coal-bearing structures (the northern structure is Bao Dai – Yen Tu and southern structure is the Hon Gai). The coal in Quang Ninh was formed in a complex geological structure with many faults and folds. There are mainly two groups of sediments in this area, viz. continental sediments and transitional sediments from continental to marine. The continental sediments are more common and account for approximately 80% of total sediments (Hien and Binh, 1966a,b).

Cam Pha coalfield is situated in the southeast of Quang Ninh coal basin, and the Coc Sau surface mine is located in the eastern part of the Cam Pha coalfield. As a result of many different phases of regional deformation, the geological structure of Cam Pha coalfield is very complex with intense folding and faulting, dividing this coalfield into many small blocks (Fig. 1) (Hung, 1997). The late Trassic Hon Gai formation is the main coal-bearing stratum in this area and unconformably underlies the lower-middle Jurassic Ha Coi formation, which is mainly composed of conglomerate, gritstone, quartz sandstone, siltstone, shale, lenses of limestone, and overlies the Carboniferous-Permian Bac Son formation which is mainly made up of thick-bedded to massive grey to light grey limestone, oolitic limestone, marl, cherty limestone.

Base on the lithological characteristics, the Hon Gai formation formed mostly under continental environment and is divided into three sections from bottom to top: the lower, middle, and upper sections, respectively (Fig. 2) (Hung, 1997). The lower section (average thickness about 300 m) is primarily made up of conglomerates, gritstones, sandstones, siltstones, and interbedded by thin lenses of coaly clays and clay flints. The middle section has the greatest thickness ranging from 1400 to 1950 m, which increases from south to north and from west to east. The middle section is mainly made up of conglomerates, sandstones, siltstones, claystones, coaly clays and consists of three main workable coal seams in the middle section, namely GII, GIII, and GIV from bottom to top, respectively. The upper section is composed of conglomerates, quartz siltstone, and interbedded by sandstone, thin layers of claystone, thin coal seams or coaly clay.

**Table 1**
Proximate analysis results of coals and non-coal rocks in the Coc Sau surface mine.

| Sample | Thickness (m) | $M_{ad}$ | $A_{ad}$ | $V_{daf}$ |
|---|---|---|---|---|
| Day-25 | 1.0 | – | 66.5 | – |
| Day-24 | 1.0 | 1.28 | 32.0 | 9.7 |
| Day-23 | 1.0 | 1.55 | 30.6 | 8.5 |
| Day-22 | 1.0 | 1.44 | 25.0 | 8.0 |
| Day-21 | 1.0 | 2.88 | 7.9 | 5.7 |
| Day-20 | 1.0 | 1.7 | 9.1 | 6.6 |
| Day-33 | 0.8 | – | 84.3 | – |
| Day-32 | 1.0 | 2.73 | 48.1 | 11.5 |
| Day-31 | 1.0 | 2.74 | 45.2 | 11.5 |
| Day-30 | 1.0 | 1.33 | 31.2 | 9.2 |
| Day-29 | 1.0 | 1.03 | 27.9 | 10.9 |
| Day-28 | 1.0 | 2.9 | 11.8 | 6.5 |
| Day-27 | 1.0 | 1.75 | 15.3 | 7.0 |
| Day-26 | 1.0 | 1.54 | 29.1 | 8.3 |
| Day-18 | 0.75 | | 56.6 | 11.3- |
| Day-17 | 0.75 | 5.92- | 57.8 | 3.0- |
| Day-16 | 0.75 | 1.3- | 54.1 | 13.5- |
| Day-15 | 0.75 | 1.12 | 20.0 | 10.0 |
| Day-14 | 0.75 | 1.23 | 30.4 | 7.9 |
| Day-13 | 0.75 | 1.49 | 21.2 | 7.3 |
| Day-12 | 0.75 | 1.45 | 13.1 | 6.1 |
| Day-11 | 0.75 | 1.5 | 12.3 | 6.2 |
| Day-10 | 0.75 | – | 91.4 | – |
| Day-9 | 1.0 | 1.69 | 28.0 | 7.4 |
| Day-8 | 1.0 | 1.41 | 26.0 | 6.7 |
| Day-7 | 0.3 | – | 89.2 | – |
| Day-6 | 1.0 | 1.18- | 52.7 | 12.6- |
| Day-5 | 1.0 | 1.79 | 17.9 | 6.7 |
| Day-4 | 1.0 | 2.06 | 6.5 | 5.5 |
| Day-3 | 1.0 | 1.65 | 37.6 | 8.7 |
| Day-2 | 1.0 | 0.99- | 54.8 | 10.7- |
| Day-1 | 1.0 | – | 79.4 | – |

## 3. Methodology

A total of thirty-two channel samples (including one roof, one floor, three parting, and twenty-seventh coal samples, numbered with prefix Day) were collected using channel profile sampling method from the GII coal seam in the Coc Sau surface mine, Cam Pha coalfield, Quang Ninh Province (Fig. 2). These samples were homogenized by using quartering and coning method, crushed, and milled to pass through 80-mesh sieves for proximate analysis and pass through 200-mesh sieves for geochemical and mineralogical analyses.

The proximate analyses of coal and host rock (parting, roof and floor) samples were carried out following the ASTM Standard D3173-11 (2011), D3174-11 (2011), and D3175-11 (2011). The mineralogical analyses were conducted using Powder X-ray diffraction (XRD) equipped with a Bruker D5005 diffractometer and monochromatic Cu Kα radiation. Scanning was done over the 2θ range of 4–60°, with a step size of 0.05° and counting time of 3 s/step. The semi-quantitative XRD analyses were estimated using the Reference Internal Standard Method (Chung, 1974). The morphology and modes of occurrence of typical minerals were observed by means of scanning electron microscope equipped with energy dispersive X-ray spectrometer (SEM-EDX).

Prior to geochemical analyses, the coal and host rock samples were first subjected to a two-step acid digestion proposed by Querol et al. (1997). Whereafter, concentrations of major and trace elements were respectively analyzed by inductively coupled plasma atomic-emission spectrometer (ICP-AES) and inductively coupled plasma mass spectrometer (ICP-MS). The accuracy of the analytical methods was checked by the Certified Reference material (SARM-19) and blank samples. Note that due to the formation of highly volatile SiF6 during the digestion process and the consequent Si loss, Si concentrations were calculated through a mass balance method, combining the mineralogical and geochemical data, using Al as a reference (Li et al., 2012). The accuracy of this method was evaluated by the correlation of calculated Al

**Table 2**
Compositions and contents (%) of mineral matter of coal and non-coal rocks from Coc Sau surface mine.

| Sample | Muscovite | Illite | Kaolinite | Clinochlore | Quartz | Ankerite | Calcite | Siderite | Pyrite | Tobellite | Anatase |
|---|---|---|---|---|---|---|---|---|---|---|---|
| Day-25 | 6.24 | <dl | 23.37 | <dl | 35.94 | 0.91 | <dl | <dl | <dl | <dl | 0.02 |
| Day-24 | 2.85 | <dl | 12.62 | <dl | 12.22 | 0.71 | <dl | <dl | <dl | 3.56 | <dl |
| Day-23 | 2.12 | <dl | 9.89 | <dl | 14.28 | 0.72 | <dl | <dl | <dl | 3.61 | <dl |
| Day-22 | 1.52 | <dl | 5.32 | 1.01 | 14.19 | 0.81 | <dl | <dl | <dl | 2.03 | 0.14 |
| Day-21 | 0.03 | <dl | 3.12 | <dl | 1.79 | 1.13 | 1.79 | <dl | <dl | <dl | <dl |
| Day-20 | 0.36 | <dl | 2.86 | <dl | 2.62 | 1.70 | 0.69 | <dl | <dl | 0.87 | <dl |
| Day-33 | 2.94 | 1.36 | 16.69 | <dl | 62.97 | <dl | <dl | <dl | <dl | <dl | 0.31 |
| Day-32 | 4.38 | <dl | 9.70 | 2.02 | 30.32 | 1.35 | <dl | <dl | <dl | <dl | 0.36 |
| Day-31 | 4.06 | <dl | 19.39 | <dl | 21.36 | 0.27 | <dl | <dl | <dl | <dl | 0.11 |
| Day-30 | 2.93 | <dl | 15.52 | <dl | 11.73 | 0.75 | 0.24 | <dl | <dl | <dl | <dl |
| Day-29 | 1.87 | <dl | 1.04 | 3.46 | 10.39 | 2.56 | <dl | 3.74 | 0.69 | 3.88 | 0.27 |
| Day-28 | 0.96 | <dl | 5.13 | <dl | 4.82 | 0.87 | <dl | <dl | <dl | <dl | <dl |
| Day-27 | 1.43 | <dl | 3.20 | 1.00 | 6.77 | 0.57 | 0.25 | <dl | <dl | 2.00 | 0.06 |
| Day-26 | 3.36 | <dl | 6.37 | <dl | 12.57 | 0.58 | <dl | <dl | <dl | 6.20 | <dl |
| Day-18 | 12.02 | 3.21 | 7.69 | <dl | 33.66 | <dl | <dl | <dl | <dl | <dl | <dl |
| Day-17 | 6.75 | <dl | 12.83 | <dl | 38.26 | <dl | <dl | <dl | <dl | <dl | <dl |
| Day-16 | 5.38 | <dl | 6.88 | 1.43 | 34.41 | <dl | <dl | <dl | <dl | 5.74 | 0.22 |
| Day-15 | 2.24 | <dl | 3.17 | 1.27 | 7.83 | 0.13 | 0.19 | <dl | <dl | 5.08 | 0.08 |
| Day-14 | 3.59 | <dl | 5.38 | 1.22 | 13.05 | <dl | <dl | <dl | <dl | 7.01 | 0.12 |
| Day-13 | 1.62 | <dl | 3.89 | 0.46 | 10.92 | 1.16 | 0.62 | <dl | <dl | 2.50 | <dl |
| Day-12 | <dl | <dl | 8.10 | 2.14 | 0.93 | 0.47 | 1.26 | <dl | <dl | <dl | 0.21 |
| Day-11 | 0.92 | <dl | 2.77 | <dl | 6.15 | 0.65 | 0.51 | <dl | <dl | 1.30 | <dl |
| Day-10 | 9.50 | <dl | <dl | 1.61 | 57.38 | 1.08 | <dl | <dl | <dl | 21.87 | <dl |
| Day-9 | 2.97 | <dl | 7.42 | <dl | 12.56 | 0.08 | <dl | <dl | <dl | 4.95 | <dl |
| Day-8 | 2.44 | <dl | 5.15 | 0.90 | 16.71 | 0.63 | <dl | <dl | <dl | <dl | 0.11 |
| Day-7 | 6.78 | <dl | <dl | 1.82 | 65.15 | <dl | <dl | <dl | <dl | 15.18 | 0.27 |
| Day-6 | 6.19 | <dl | 6.55 | 1.60 | 30.57 | <dl | 0.33 | <dl | <dl | 7.28 | 0.15 |
| Day-5 | 0.81 | <dl | 6.30 | 1.79 | 6.55 | 0.14 | 0.53 | <dl | <dl | 1.68 | 0.08 |
| Day-4 | <dl | <dl | 3.70 | 1.00 | 0.20 | 0.37 | 1.20 | <dl | <dl | <dl | <dl |
| Day-3 | 2.47 | <dl | 23.16 | 1.03 | 9.42 | 0.72 | 0.46 | <dl | <dl | <dl | 0.34 |
| Day-2 | 7.46 | <dl | 4.97 | <dl | 42.29 | <dl | <dl | <dl | <dl | <dl | 0.07 |
| Day-1 | 11.34 | <dl | 15.24 | <dl | 52.62 | <dl | <dl | <dl | <dl | <dl | 0.19 |

<dl, below detection limit of XRD.

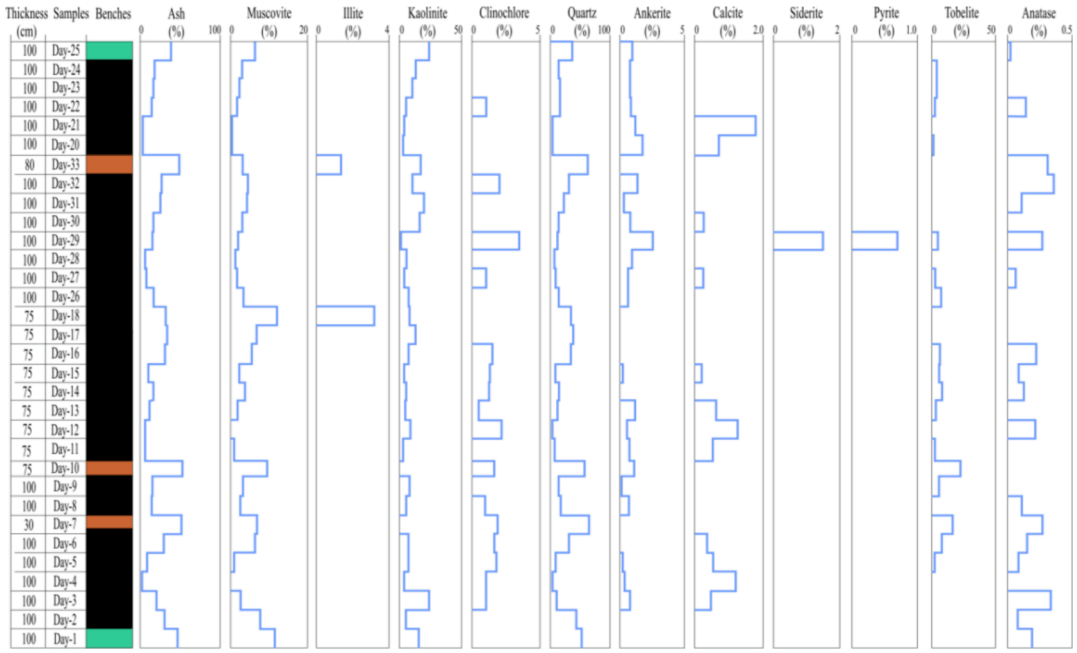


**Fig. 3.** Vertical variations of minerals in GII coal seam from Coc Sau surface mine.

concentration with that determined by ICP-AES.

The SPSS statistical program was used to perform statistical analyses of the geochemical data. The elemental affinities were evaluated by means of the Pearson's correlation analysis between trace element concentrations and ash yields as well as some major element (Al, Si, Fe, S, Ca, Mg) concentrations representative of different mineral phases. In the current research, with a statistical sample number of 32, the Pearson's correlation coefficients are significant at a level of 0.01 ($p < 0.01$).

## 4. Results

### 4.1. Coal characterization

The proximate analysis results of the studied samples from the Coc Sau mine are given in Table 1. The moisture contents and ash yields of Coc Sau coals respectively range from 1.0% to 5.9% (on air dry basis, avg. 1.8%) and from 6.5% to 57.8% (on dry basis, avg. 29.7%). The volatile matter content of the coal samples vary between 3.0% and 13.5% (on dry and ash-free basis), with an average of 8.4%, indicating that the late Triassic coals in Coc Sau mine reached semianthracite rank (ASTM D388 -12, 2012).

### 4.2. Coal mineralogy

#### 4.2.1. Mineral composition

The composition and semi-quantitative contents of minerals in the Coc Sau coals and non-coals (roof, floor and parting) are shown in Table 2. The mineralogy of the coal benches is dominantly composed of quartz (avg. 15.1%), kaolinite (7.5%), with minor proportions of muscovite (3.0%) and tobelite (2.1%). Ankerite, anatase, clinochlore, and calcite were also detected with minor and trace amounts in some samples. Siderite and pyrite were identified in only one sample (Day-29).

The main mineral assemblages present in roof, floor, and parting samples are similar to those in the coals, dominated by quartz (55.4% on average), kaolinite (10.0%), and to lesser extent, muscovite (6.4%), along with minor proportions of tobelite, ankerite, illite and anatase.

#### 4.2.2. Distribution and occurrence of minerals

*4.2.2.1. Aluminosilicate minerals.* Kaolinite is a relative abundant mineral widely distributed in the whole GII coal seam except in the gangue samples (Day7 and Day10) in the lower coal seam where kaolinite was not detected by XRD (Fig. 3). Kaolinite is mainly distributed as laminar layers in coal matrix (Fig. 4a), or occurs as fracture-infillings in coals or roof of the coals (Fig. 4b, Fig. 5c), which respectively indicates a detrital and authigenic origin, and both are most likely derived from terrigenous fine-grained clasts. A small amount of authigenic vermicular kaolinite (Fig. 5a, b) was observed in the floor rock sample (Day1), which may be related to the epigenetic genesis of hydrothermal alteration and recrystallization of volcanic ash (Dai et al., 2017a).

Muscovite is also abundant in the studied coals and widely distributed in the whole GII coal seam with the exception of two coal samples (Day4 and Day12) in the lower coal section (Fig. 3). Muscovite is found distributed in the form of matrix-infillings (Fig. 4c-e) or fragments (Fig. 6a, e) in coal. The contents of muscovite in non-coal rocks (roof/floor/parting) are much higher than in the coal samples (Table 2). Both muscovite and kaolinite have similar vertical distribution with ash yield (Fig. 3), suggesting the occurrence of these minerals are influenced by the similar terrigenous sources and geological environmental condition (Hien and Binh, 1966a,b).

Illite was only detected in samples of parting (Day-33) and high-ash coal (Day-18) by XRD (Fig. 7). The mixed layer of illite and muscovite was observed under SEM (Fig. 6a), which indicates an authigenic origin weathering from muscovite.

Tobelite is widely distributed in the coal seam and has a relatively

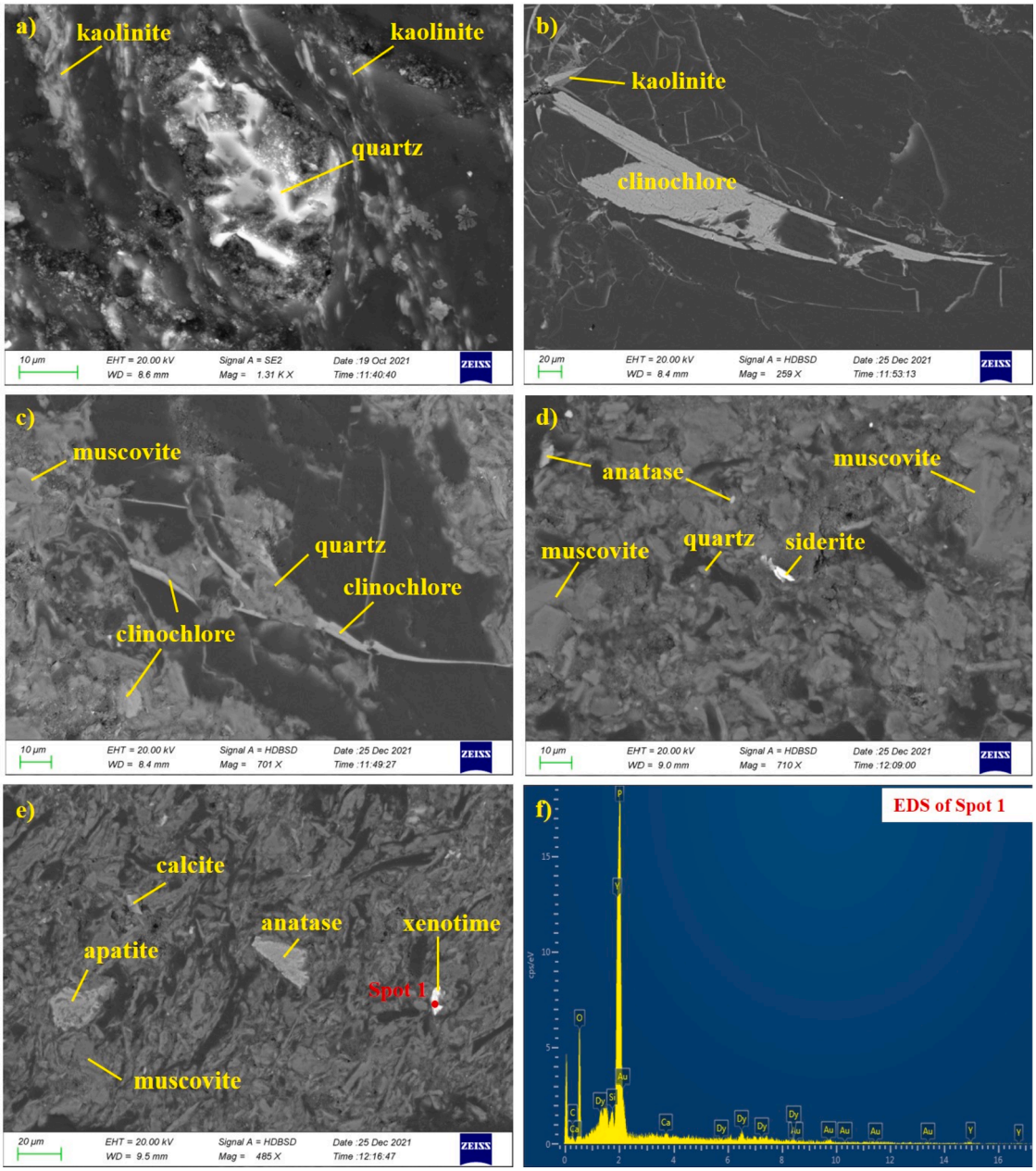


**Fig. 4.** SEM images of minerals in the Coc Sau coals. a) laminar layers of micron-sized kaolinite and fine-grained siliceous debris; b) fracture-filling kaolinite and clinochlore; c) micron-sized quartz and fracture-filling clinochlore; d) Fine-grained siliceous debris, and discrete particles of siderite, and anatase; e) Laminar layers of muscovite and discrete crystals of apatite, anatase and xenotime; f) EDS of xenotime.

high content in two partings (Day-7 and Day-10) in lower coal seams and absent in in roof and floor samples (Fig. 3). Tobelite have previously been found in some coals in Chongqing (Dai et al., 2017b) and Shaanxi (Li et al., 2020) in China, as well as in South Walker, Australia (Permana et al., 2013). It was reported that tobelite in coal is formed by interaction between kaolinite and $NH_4^+$ released from organic matter under high-temperature conditions (>200 °C) during rank advance or during hydrothermal alteration (Boudou et al., 2008; Permana et al., 2013; Dai et al., 2017b). In addition, clinochlore is widely distributed in the middle and lower portion of coal seam, but was not detected in the roof and floor samples (Fig. 3). Clinochlore occurs in the form of fracture infillings (Fig. 4b, c) in the coal samples, which indicates that clinochlore was formed during epigenetic hydrothermal alteration.

*4.2.2.2. Oxide minerals.* Quartz is the most abundant mineral in the coal and non-coal samples and widely distributed in the whole GII coal seam (Fig. 3). Quartz was found occurring as discrete fine-grained siliceous particles and quartz grains in the coals (Fig. 4a, c, d). In the non-coal rock of the GII coal seam, quartz occurs as a fracture-infilling form (Fig. 5d), representing an authigenic and epigenetic origin. Furthermore, the vertical distribution of quartz is very similar to that of muscovite in the coal seam (Fig. 3), indicating the similar terrigenous sources with muscovite.

Anatase is widely distributed in coal seams and occurs as anhedral crystals (Fig. 4d, e; Fig. 5a, c, f) in both coals and non-coal rocks, indicating an authigenic process for formation of anatase.

*4.2.2.3. Carbonate minerals.* Ankerite is widely distributed in coal

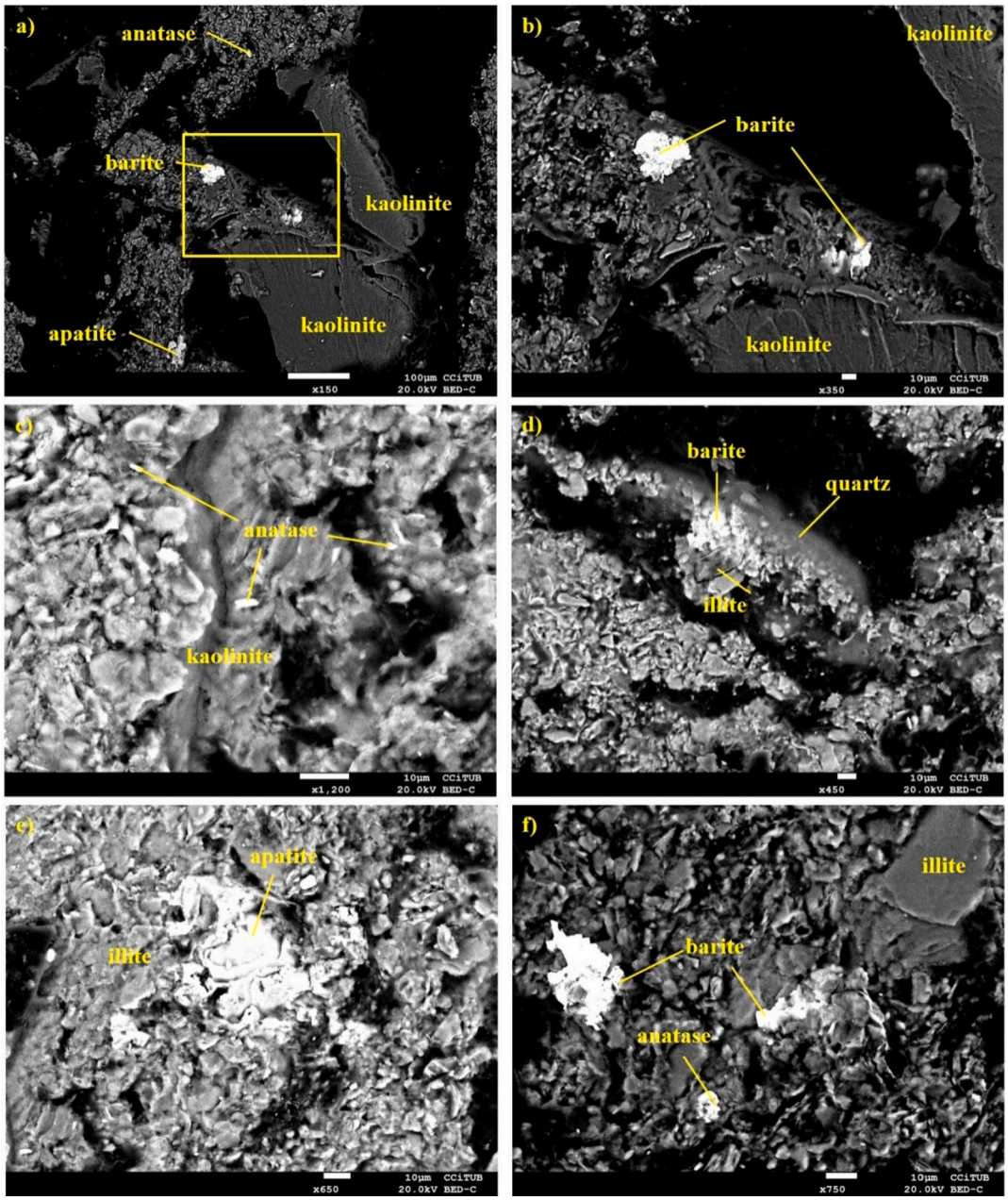


**Fig. 5.** SEM back-scattered electron images of minerals in the non-coal rock of the Coc Sau coals. a) Vermicular kaolinite and euhedral crystals of barite, anatase, and apatite; b) Enlargement of yellow rectangle in (a); c) Kaolinite and euhedral crystals of anatase; d) Quartz, barite and illite, fracture-infilling minerals; e) Euhedral crystals of apatite, illite; f) Euhedral crystals of anatase and bariteas. illite, day1. (For interpretation of the references to colour in this figure legend, the reader is referred to the web version of this article.)

seams and occurs with higher proportions in most coal bench samples relative to the host rocks and high ash coals (Fig. 3). Calcite is intermittently distributed in coal seams and absent in the host rocks (Fig. 3), occurring as fracture-infilling veins in some coals (Fig. 6d), indicating its epigenetic origin. It was precipitated from Ca-rich solutions infiltrated the coal seam through extensive cleat/fracture system but could not penetrate into non-coal rocks due to low permeability after late diagenesis. Siderite occasionally occurs as anhedral crystals in Coc Sau coals (Fig. 4d), reflecting an authigenic origin.

*4.2.2.4. Other minerals.* Although not detected by XRD, euhedral zircon grain was found occurring in the Coc Sau coals by SEM-EDX observation (Fig. 6b, c, e), and was partially corroded (Fig. 6c), which most likely derived from a detrital origin. Furthermore, trace amounts of rare earth element-bearing minerals such as xenotime (Fig. 4e, f) and florencite (Fig. 6e, f), also occur as discrete fine grains, indicating a detrital origin as well. In addition, minor proportions of barite and apatite were sporadically observed by SEM-EDX in the non-coal rocks, occurring as subhedral crystals or assemblages (Fig. 5a-b, d-e), representing an authigenic origin.

### 4.3. Coal geochemistry

#### 4.3.1. Major and trace element concentrations

The concentrations of major and trace elements in the coal and non-coal rock samples, together with the average values of world coals

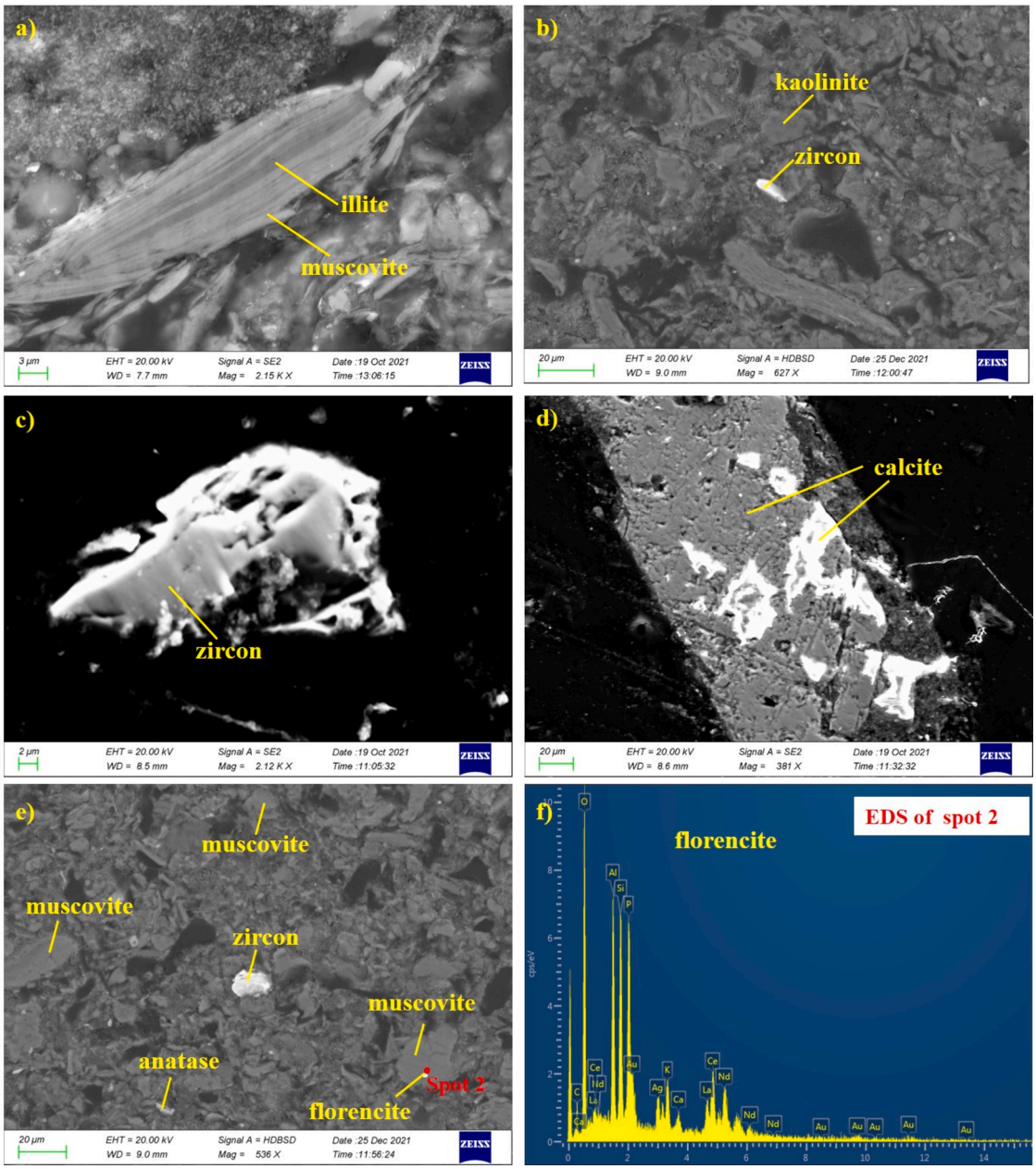


**Fig. 6.** SEM images of minerals in the Coc Sau coals. a) muscovite and illite occurring as fragments; b) kaolinite and zircon grains; c) partially dissolved zircon: d) Calcite vein: e) muscovite fragments, zircon and anatase grains, and corpuscular florencite: f) EDS of florencite.

reported by Ketris and Yudovich (2009) are listed in Table 3.

The major element concentrations in Coc Sau coal are dominated by Si (avg. 9.94%) and Al (3.59%) and to a lesser extent of K and Fe. Aluminum, Si, K, Mg, and Na have significant correlations with ash yield ($r = 0.77–0.89$), which indicates that these elements occur primarily in mineral matter, such as clay minerals.

According to the concentration coefficient (CC, the ratio of trace element concentration in the studied coal versus the corresponding average value of world hard coals) proposed by Dai et al. (2015a,b,c), Cs (9.4 mg/kg) and Rb (89.2 mg/kg) are highly enriched ($5 < CC < 10$) in the Coc Sau coal. Elements including V (51.2 mg/kg), Cr (39.0 mg/kg), Pb (24.6 mg/kg), and Th (9.6 mg/kg) are slightly enriched (with $2 < CC < 5$), while the remaining elements in the Coc Sau coal are similar or depleted relative to the averages of world hard coals (Ketris and Yudovich, 2009, Fig. 8).

The total REY concentrations of Coc Sau coals are from 32.0 to 204 mg/kg (avg. 99.3 mg/kg, Table 3), which are higher than the average REY concentration of world hard coals (67.9 mg/kg, Ketris and Yudovich, 2009). According to the three fold classification of REY, REY in the Coc Sau coal and host rock samples are characterized by high LREY concentrations, pointing to a LREY enrichment pattern (Seredin and Dai, 2012).

### 4.3.2. *Modes of occurrence of trace elements*

1) Aluminosilicate affinity. Most of trace elements including Li, Be, B, Sc, Ti, V, Cr, Ga, Ge, Rb, Sr, Y, Nb, Sn, Cs, Ba, Ta, W, Tl, Th, and U in the investigated coals have positive correlation coefficients with Al ($r = 0.67–0.98$) and ash yield ($r = 0.74–0.96$), pointing to an aluminosilicate

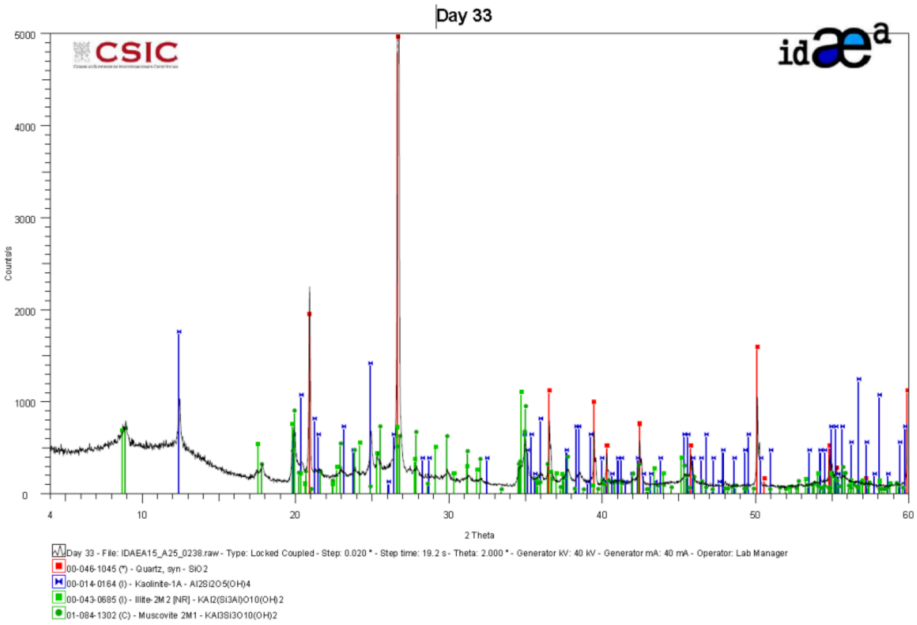


**Fig. 7.** XRD spectrum of illite, muscovite and other minerals in the coal parting sample (Day 33) of the Coc Sau coals.

affinity for these elements, which are most likely associated with clay minerals such as kaolinite, and muscovite in Coc Sau coals (Fig. 9). Hf, Nb, Th, and Ta are remarkably positively correlated with Zr (r = 0.92–0.99) and Ti (r = 0.91–0.97), indicating that they probably occur in zircon. REY is also highly correlated with ash yield (r = 0.89), Al (r = 0.96), and Si content (r = 0.89), inferring that REY in this studied coal are largely characterized by inorganic affinity, mainly associated with clay minerals, and to some extent occur in REY-bearing minerals, e.g., xenotime and florencite as aforementioned.

2) Phosphate affinity. The positive correlation between P and Sr (r = 0.76), P and Ba (r = 0.60), as well as P and Ce (r = 0.64), suggests a phosphate affinity. Strontium, Ba, and Ce may occur in apatite in the studied coals, which agrees with previous research (Ward, 2002; Yang et al., 2016).

3) Carbonate affinity. The obviously positive correlation between Mn and Fe (r = 0.91) indicates that Mn probably occurs in carbonate minerals such as siderite and ankerite, which were detected in the investigated coals.

4) Organic affinity. Arsenic is highly correlated with sulfur (r = 0.72) and partially negatively correlated with ash yield (r = −0.48) in the studied coals, suggesting that As is organically associated in the Coc Sau coal. In addition, the negative correlation of Co with Al (r = −0.76) and ash yield (r = −0.79) suggests that Co is probably associated with organic matter in the Coc Sau coal, which is consistent with previous studies (Dai et al., 2013a,b; Swaine, 1990).

## 5. Discussion

### 5.1. Depositional environment

Boron and S are the two elements that are widely used for specific coal-forming environments (Dai et al., 2015a,b,c; Goodarzi and Gentzis, 1987; Goodarzi and Swaine, 1994). Coals formed in fresh water environments are generally characterized by low pyrite contents, high kaolinite, and low total sulfur (<0.6%) content (Banerjee and Goodarzi, 1990). The sulfur contents in the studied coals are very low (from 0.01% to 0.28%, except that in Day-29 sample of 0.71%, Fig. 10). Furthermore, pyrite content is also low in the Coc Sau coals, occurring with trace amount (0.68%) in only one sample (Day-29, Table 3). The low pyrite and low total sulfur contents indicate that the studied coals were formed mostly under continental environment (Banerjee and Goodarzi, 1990; Hung, 1997).

Boron concentration in coal is unaffected by age and coal rank and would be used to define the degree of marine influence during the early stages of coalification. The values of B content less than 50 mg/kg indicate the fresh water-influenced environments, while B content between 50 and 110 mg/kg points to the mildly brackish-water influenced environment, and B content higher than 110 mg/kg is indicative of brackish-water influenced environment (Goodarzi and Swaine, 1994). With exception of the parting samples (Day-10 and Day-33) and two coal samples (Day-2 and Day-3) adjacent to the roof of which B concentrations are higher than 110 mg/kg, B concentrations in the remaining coal samples are largely lower than 50 mg/kg or at least lower than 110 mg/kg (Fig. 10). The average B content in this investigated coal is about 18.03 mg/kg and indicates fresh water-influenced coal-forming environments. The higher concentration of boron in the aforementioned coal and parting samples than in other coal samples may be due to the slight change of pH, Eh or depositional environment conditions (Goodarzi and Swaine, 1994).

In addition, Sr/Ba ratio ratio is widely used as an indicator for ambient water, in terms of seawater and freshwater and their mixtures (Schmitz et al., 1991; Arai and Hirata, 2006), and consequently is indicative of a seawater/freshwater effect in coal and coal host rocks (Chen et al., 2015; Dai et al., 2013a,b; Spiro et al., 2019; Yan et al., 2019). Spiro et al. (2019) reported a general negative correlation between Sr/Ba ratio and ash yield in coal, and clarified that the boundary at Sr/Ba = 1.0 provides a criterion as a marine/freshwater indicator. In this study, all of coal and non-coal samples have Sr/Ba ratio less than 1 (Fig. 10, varying from 0.06 to 0.92 in coal and from 0.08 to 0.19 in non-coal rocks, respectively), indicating the fresh water-influenced environments during coal formation. The relatively higher Sr/Ba ratio is vertically in accordance with the higher B concentration, which is also probably ascribed to changes of pH, Eh or depositional environment conditions (Goodarzi and Swaine, 1994).

Based on the valuation and distribution of boron and sulfur contents as well as the ratio of Sr/Ba, it is obvious that the Coc Sau coals were

**Table 3**
The contents of major elements and trace elements in coal and non-coal rocks from Coc Sau coal mine compared to worldwide coals (on whole-coal basis).

| | Day-25 | Day-24 | Day-23 | Day-22 | Day-21 | Day-20 | Day-33 | Day-32 | Day-31 | Day-30 | Day-29 | Day-28 | Day-27 | Day-26 | Day-18 | Day-17 | World[a] |
|---|---|---|---|---|---|---|---|---|---|---|---|---|---|---|---|---|---|
| Si* | 23.23 | 9.89 | 10.12 | 8.73 | 1.52 | 2.13 | 34.08 | 17.52 | 15.08 | 9.49 | 6.87 | 3.57 | 4.77 | 9.41 | 20.78 | 22.13 | |
| Al* | 9.12 | 4.17 | 3.79 | 3.21 | 1.08 | 1.49 | 11.20 | 3.45 | 5.22 | 4.70 | 2.19 | 1.50 | 2.11 | 4.22 | 9.04 | 8.43 | |
| Ca* | 0.33 | 0.37 | 0.25 | 0.27 | 0.68 | 0.49 | 0.10 | 0.49 | 0.24 | 0.39 | 0.60 | 0.26 | 0.27 | 0.35 | 0.10 | 0.13 | |
| Fe* | 0.89 | 0.66 | 0.44 | 0.66 | 0.25 | 0.33 | 0.65 | 0.74 | 0.74 | 0.61 | 3.46 | 0.58 | 0.68 | 0.66 | 0.62 | 0.72 | |
| K* | 1.63 | 0.98 | 0.75 | 0.60 | 0.12 | 0.23 | 2.37 | 0.93 | 1.18 | 1.09 | 0.58 | 0.31 | 0.45 | 1.02 | 3.09 | 2.45 | |
| Mg* | 0.32 | 0.26 | 0.18 | 0.14 | 0.10 | 0.15 | 0.41 | 0.28 | 0.27 | 0.25 | 0.39 | 0.14 | 0.17 | 0.27 | 0.44 | 0.38 | |
| Na* | 0.06 | 0.03 | 0.03 | 0.03 | 0.01 | 0.02 | 0.09 | 0.03 | 0.04 | 0.03 | 0.01 | 0.01 | 0.01 | 0.03 | 0.12 | 0.60 | |
| S* | 0.08 | 0.18 | 0.23 | 0.23 | 0.28 | 0.27 | 0.04 | 0.08 | 0.13 | 0.19 | 0.71 | 0.25 | 0.23 | 0.24 | 0.12 | 0.13 | |
| Li | 74.4 | 31.0 | 27.9 | 26.6 | 11.8 | 9.9 | 113.1 | 36.7 | 44.0 | 31.2 | 12.2 | 6.4 | 9.5 | 13.4 | 14.2 | 36.5 | 12 |
| Be | 3.0 | 1.7 | 1.3 | 1.3 | <dl | <dl | 3.8 | 1.6 | 2.8 | 1.8 | 0.8 | <dl | <dl | 1.6 | 3.4 | 2.3 | 1.6 |
| B | 31.8 | 10.2 | 49.5 | 36.0 | 20.1 | 35.6 | 144.9 | 50.2 | 52.5 | 54.8 | 36.3 | 10.9 | 33.2 | 70.5 | 25.7 | 18.6 | 52 |
| P | 319 | 194 | 201 | 288 | 32 | 79 | 203 | 176 | 184 | 403 | 84 | 89 | 50 | 76 | 318 | 224 | 231 |
| Sc | 17.1 | 8.6 | 7.0 | 5.8 | <dl | <dl | 28.4 | 5.1 | 13.9 | 9.4 | <dl | 2.3 | 4.7 | 9.4 | 19 | 18 | 3.9 |
| Ti | 3270 | 2038 | 1649 | 1231 | 286 | 533 | 6640 | 1790 | 2330 | 1717 | 1196 | 648 | 869 | 1756 | 3615 | 3266 | 798 |
| V | 98.9 | 54.2 | 59.2 | 59.0 | 19.8 | 21.2 | 130.4 | 53.6 | 82.6 | 61.8 | 29.7 | 34.3 | 36.4 | 51.0 | 114 | 112 | 25 |
| Cr | 72.1 | 47.3 | 42.8 | 35.0 | 13.7 | 15.2 | 116.2 | 38.0 | 60.0 | 48.6 | 25.1 | 25.7 | 29.7 | 45.4 | 84.6 | 80.8 | 16 |
| Mn | 48.1 | 40.3 | 20.4 | 25.7 | 25.4 | 27.6 | 19.8 | 37.4 | 46.8 | 33.5 | 226.0 | 33.1 | 39.2 | 48.1 | 27.2 | 36.8 | 85 |
| Co | 3.6 | 6.8 | 8.9 | 5.3 | 6.4 | 6.7 | 3.8 | 5.5 | 7.2 | 10.2 | 8.9 | 8.7 | 7.0 | 7.7 | 5.1 | 4.0 | 5.1 |
| Ni | 16.1 | 15.7 | 17.0 | 13.4 | 11.4 | 13.3 | 23.5 | 11.9 | 20.7 | 18.1 | 14.8 | 16.7 | 15.8 | 34.1 | 15.6 | 28.2 | 13 |
| Cu | 24.0 | 15.8 | 26.0 | 39.8 | 24.1 | 7.8 | 66.0 | 25.6 | 50.9 | 37.8 | 19.9 | 9.8 | 16.6 | 13.8 | 1.3 | 17.0 | 16 |
| Zn | 27.5 | 23.3 | 25.8 | 25.2 | 36.7 | 32.2 | 26.9 | 19.7 | 63.4 | 27.6 | 25.4 | 19.8 | 33.8 | 72.3 | 22.2 | 400.7 | 23 |
| Ga | 24.9 | 14.4 | 11.8 | 9.8 | 2.9 | 3.8 | 38.4 | 11.4 | 17.0 | 13.5 | 6.8 | 4.2 | 7.3 | 11.8 | 23.7 | 22.3 | 5.8 |
| Ge | 2.3 | 1.6 | 1.4 | 1.2 | <dl | <dl | 3.3 | 1.0 | 1.7 | 1.3 | <dl | <dl | <dl | 1.3 | 2.1 | 2.1 | 2.2 |
| As | 5.1 | 13.6 | 13.6 | 10.0 | 10.4 | 10.3 | 7.5 | 6.8 | 7.2 | 13.4 | 18.2 | 10.0 | 8.4 | 10.8 | 6.8 | 3.7 | 8.3 |
| Se | <dl | <dl | <dl | <dl | <dl | <dl | <dl | <dl | <dl | <dl | <dl | <dl | <dl | <dl | 2.5 | 2.9 | 1.3 |
| Rb | 162 | 112 | 83.9 | 78.1 | 15.7 | 25.7 | 259 | 95.5 | 125 | 111 | 57.2 | 27.0 | 54.2 | 114 | 275.4 | 181.0 | 14 |
| Sr | 68.3 | 37.1 | 22.0 | 21.3 | 8.3 | 8.2 | 62.6 | 24.8 | 33.2 | 33.5 | 13.0 | 18.4 | 14.0 | 23.0 | 43 | 41 | 110 |
| Y | 21.4 | 13.7 | 13.6 | 12.2 | 6.3 | 6.3 | 31.3 | 12.1 | 22.1 | 14.9 | 7.7 | 9.1 | 7.9 | 11.4 | 27.3 | 24.1 | 8.4 |
| Zr | 87.5 | 55.1 | 45.2 | 33.6 | 8.8 | 12.0 | 174.7 | 49.6 | 69.1 | 41.8 | 23.2 | 13.4 | 19.2 | 41.7 | 77.9 | 113.4 | 36 |
| Nb | 15.9 | 9.3 | 7.3 | 5.4 | 1.5 | 2.1 | 29.6 | 8.2 | 11.1 | 7.8 | 4.2 | 2.1 | 3.8 | 7.1 | 11.1 | 10.4 | 3.7 |
| Mo | 1.1 | <dl | 1.5 | 1.5 | 1.2 | <dl | <dl | <dl | 1.2 | 1.9 | <dl | 1.0 | 0.9 | <dl | <dl | 1.1 | 2.2 |
| Sn | 5.6 | 2.5 | 2.1 | 1.7 | 0.6 | 0.5 | 7.6 | 2.2 | 3.4 | 2.7 | 1.1 | 0.9 | 0.8 | 1.9 | 4.6 | 4.2 | 1.1 |
| Sb | 2.0 | 1.3 | 2.4 | 1.6 | 2.0 | 1.3 | 3.3 | 1.0 | 4.4 | 3.1 | 3.7 | 0.9 | 1.9 | 1.6 | 0.8 | 1.9 | 0.92 |
| Cs | 30.9 | 17.0 | 13.3 | 11.2 | 2.3 | 3.7 | 68.1 | 16.0 | 22.6 | 13.8 | 7.1 | 2.8 | 5.4 | 10.7 | 23.1 | 14.4 | 1 |
| Ba | 368 | 226 | 191 | 163 | 51 | 81 | 591 | 207 | 280 | 295 | 134 | 74 | 113 | 226 | 737.6 | 541.0 | 150 |
| La | 37.4 | 25.3 | 20.0 | 17.6 | 4.9 | 7.1 | 56.7 | 22.1 | 29.0 | 23.5 | 12.2 | 12.0 | 9.1 | 19.4 | 34 | 34 | 11 |
| Ce | 78.8 | 45.9 | 37.6 | 36.5 | 10.9 | 15.7 | 111.3 | 38.1 | 53.9 | 46.7 | 18.0 | 20.4 | 18.0 | 40.7 | 69.8 | 63.5 | 23 |
| Pr | 8.1 | 5.2 | 4.2 | 3.6 | 1.2 | 1.6 | 11.2 | 4.6 | 6.0 | 4.7 | 2.4 | 1.8 | 1.8 | 4.1 | 8.0 | 7.2 | 3.5 |
| Nd | 29.5 | 20.2 | 16.1 | 13.3 | 4.7 | 6.5 | 40.0 | 16.9 | 21.9 | 16.9 | 8.9 | 5.8 | 6.7 | 15.4 | 28.2 | 26.0 | 12 |
| Sm | 6.8 | 4.7 | 3.8 | 3.3 | 1.4 | 1.6 | 7.7 | 3.9 | 5.5 | 3.7 | 2.2 | 1.9 | 1.9 | 3.8 | 5.0 | 4.8 | 2 |
| Eu | 0.9 | <dl | <dl | <dl | <dl | <dl | 1.1 | <dl | 0.8 | <dl | <dl | <dl | <dl | <dl | 1.0 | 1.0 | 0.47 |
| Gd | 5.4 | 3.7 | 3.2 | 3.2 | 1.3 | 1.6 | 6.1 | 3.1 | 4.8 | 3.6 | 1.9 | 2.1 | 1.7 | 3.0 | 4.7 | 4.4 | 2.7 |
| Tb | <dl | <dl | <dl | <dl | <dl | <dl | 0.9 | <dl | <dl | <dl | <dl | <dl | <dl | <dl | <dl | <dl | 0.32 |
| Dy | 4.2 | 2.6 | 2.6 | 2.5 | 1.2 | 1.3 | 5.7 | 2.3 | 4.2 | 2.8 | 1.5 | 2.0 | 1.6 | 2.1 | 4.3 | 4.3 | 2.1 |
| Ho | 0.8 | <dl | <dl | <dl | <dl | <dl | 1.1 | <dl | <dl | <dl | <dl | <dl | <dl | <dl | 0.9 | 0.9 | 0.54 |
| Er | 2.5 | 1.6 | 1.5 | 1.4 | <dl | <dl | 3.7 | 1.4 | 2.5 | 1.6 | 0.9 | 1.0 | 0.9 | 1.3 | 2.6 | 2.5 | 0.93 |
| Yb | 2.4 | 1.5 | 1.6 | 1.3 | <dl | <dl | 3.8 | 1.4 | 2.3 | 1.6 | 0.8 | 1.0 | 0.9 | 1.3 | 2.5 | 2.4 | 1.0 |
| Hf | 3.6 | 2.2 | 1.8 | 1.4 | <dl | <dl | 6.8 | 2.0 | 2.8 | 1.7 | 0.9 | 0.0 | 0.8 | 1.6 | 2.0 | 2.8 | 1.2 |
| Ta | 1.5 | <dl | <dl | <dl | <dl | <dl | 2.8 | <dl | 0.9 | 0.0 | 0.0 | 0.0 | 0.0 | 0.0 | 1.0 | 0.9 | 0.28 |
| W | 5.5 | 1.9 | 2.2 | 1.6 | <dl | <dl | 7.0 | 2.1 | 3.1 | 2.2 | 0.8 | 0.0 | 0.8 | 1.3 | 2.2 | 1.9 | 1.1 |
| Tl | <dl | <dl | <dl | <dl | <dl | <dl | 1.4 | <dl | <dl | <dl | <dl | <dl | <dl | <dl | 1.2 | 0.8 | 0.63 |
| Pb | 36.1 | 39.3 | 24.9 | 25.1 | 49.4 | 25.0 | 12.6 | 34.6 | 44.0 | 29.8 | 30.2 | 22.7 | 28.9 | 35.8 | 3.6 | 47.3 | 7.8 |
| Bi | 1.0 | <dl | <dl | <dl | <dl | <dl | 0.9 | <dl | <dl | <dl | <dl | <dl | <dl | <dl | <dl | 1.3 | 0.97 |
| Th | 24.9 | 13.6 | 11.9 | 10.1 | 4.7 | 4.3 | 35.4 | 11.1 | 15.2 | 16.9 | 5.9 | 6.7 | 8.1 | 11.3 | 10.6 | 13.8 | 3.3 |
| U | 6.4 | 3.2 | 3.2 | 2.7 | 1.0 | 0.9 | 7.8 | 2.8 | 4.4 | 4.4 | 1.3 | 1.2 | 1.7 | 2.3 | 2.5 | 3.4 | 2.4 |

| **Sample** | **Day-16** | **Day-15** | **Day-14** | **Day-13** | **Day-12** | **Day-11** | **Day-10** | **Day-9** | **Day-8** | **Day-7** | **Day-6** | **Day-5** | **Day-4** | **Day-3** | **Day-2** | **Day-1** |
|---|---|---|---|---|---|---|---|---|---|---|---|---|---|---|---|---|
| Si* | 20.26 | 6.17 | 9.82 | 6.94 | 2.51 | 3.97 | 34.12 | 9.26 | 9.59 | 35.67 | 18.94 | 5.25 | 1.04 | 10.13 | 22.45 | 30.34 |
| Al* | 6.57 | 2.72 | 3.67 | 2.40 | 1.10 | 1.81 | 10.39 | 3.21 | 3.22 | 8.46 | 6.57 | 2.47 | 1.00 | 0.99 | 6.67 | 8.94 |
| Ca* | 0.16 | 0.19 | 0.21 | 0.45 | 0.48 | 0.35 | 0.15 | 0.18 | 0.28 | 0.13 | 0.31 | 0.30 | 0.41 | 0.36 | 0.14 | 0.24 |
| Fe* | 0.84 | 0.47 | 0.65 | 0.48 | 0.49 | 0.39 | 1.66 | 0.51 | 0.62 | 1.33 | 1.27 | 0.67 | 0.48 | 0.38 | 0.62 | 1.37 |
| K* | 2.04 | 0.78 | 1.00 | 0.58 | 0.12 | 0.35 | 3.04 | 0.97 | 0.97 | 2.94 | 2.01 | 0.47 | 0.11 | 0.11 | 2.34 | 2.71 |
| Mg* | 0.31 | 0.08 | 0.19 | 0.19 | 0.09 | 0.13 | 0.44 | 0.18 | 0.12 | 0.43 | 0.35 | 0.13 | 0.09 | 0.08 | 0.33 | 0.44 |
| Na* | 0.06 | 0.02 | 0.03 | 0.02 | <dl | 0.02 | 0.07 | 0.02 | 0.02 | 0.06 | 0.05 | 0.01 | 0.001 | 0.01 | 0.08 | 0.07 |
| S* | 0.11 | 0.17 | 0.16 | 0.17 | 0.21 | 0.20 | 0.01 | 0.13 | 0.16 | 0.02 | 0.11 | 0.16 | 0.23 | 0.21 | 0.13 | 0.07 |
| Li | 22.6 | 10.7 | 15.6 | 13.1 | 12.6 | 11.1 | 35.4 | 14.1 | 13.5 | 37.7 | 29.9 | 18.5 | 10.1 | 10.5 | 23.5 | 41.2 |
| Be | 2.2 | 1.2 | 1.4 | 1.0 | <dl | 0.9 | 3.7 | 1.6 | 1.1 | 3.0 | 2.2 | <dl | <dl | <dl | 2.2 | 3.1 |
| B | 51.2 | 43.1 | 58.1 | 51.6 | 30.7 | 47.1 | 176.4 | 6.1 | 4.8 | 79.5 | 27.7 | 57.0 | <dl | 179.4 | 411.9 | 79.9 |
| P | 422 | 111 | 140 | 92 | 331 | 113 | 451 | 205 | 158 | 385 | 411 | 252 | 270 | 269 | 188 | 301 |
| Sc | 9.8 | 4.8 | 8.6 | 3.7 | <dl | 2.6 | 22.1 | 4.3 | 4.1 | 19.1 | 12.5 | 2.2 | 3 | 3 | 14 | 21.7 |
| Ti | 2991 | 1037 | 1569 | 1043 | 340 | 695 | 5530 | 1551 | 1584 | 4995 | 3088 | 1034 | 335.3 | 322.9 | 3574.2 | 3730 |
| V | 86.4 | 43.4 | 51.6 | 32.8 | 18.1 | 24.0 | 111.0 | 51.4 | 48.9 | 108.0 | 86.6 | 33.3 | 17 | 16 | 83 | 107.1 |

(*continued on next page*)

**Table 3** (*continued*)

| Sample | Day-16 | Day-15 | Day-14 | Day-13 | Day-12 | Day-11 | Day-10 | Day-9 | Day-8 | Day-7 | Day-6 | Day-5 | Day-4 | Day-3 | Day-2 | Day-1 |
|---|---|---|---|---|---|---|---|---|---|---|---|---|---|---|---|---|
| Cr | 68.0 | 29.6 | 42.5 | 27.2 | 13.4 | 18.6 | 86.5 | 38.9 | 36.5 | 85.1 | 66.9 | 25.2 | 12.6 | 14.4 | 66.3 | 81.4 |
| Mn | 34.0 | 23.5 | 33.4 | 40.3 | 51.1 | 39.8 | 84.7 | 26.1 | 54.9 | 35.6 | 66.6 | 38.1 | 47.8 | 35.8 | 32.0 | 132.5 |
| Co | 7.1 | 7.1 | 7.3 | 6.7 | 8.4 | 6.9 | 1.9 | 6.0 | 7.5 | 2.8 | 5.2 | 8.6 | 8.4 | 7.5 | 3.7 | 3.7 |
| Ni | 21.2 | 12.9 | 16.7 | 13.3 | 13.9 | 12.7 | 10.3 | 12.3 | 22.5 | 15.1 | 15.6 | 14.6 | 14.3 | 14.5 | 26.3 | 24.6 |
| Cu | 21.4 | 14.1 | 18.6 | 12.7 | 3.7 | 12.3 | 16.3 | 16.7 | 15.2 | 23.6 | 28.3 | 9.5 | 9.9 | 14.9 | 44.7 | 29.1 |
| Zn | 39.4 | 17.6 | 20.4 | 12.6 | 13.9 | 18.8 | 23.2 | 18.2 | 18.1 | 26.3 | 25.1 | 17.2 | 28.8 | 39.5 | 56.8 | 30.5 |
| Ga | 15.2 | 8.4 | 10.9 | 6.9 | 3.0 | 5.0 | 28.3 | 10.5 | 8.5 | 26.2 | 19.4 | 7.1 | 3.0 | 3.0 | 18.9 | 24.3 |
| Ge | 1.1 | <dl | 0.8 | <dl | <dl | <dl | 2.6 | 0.9 | <dl | 2.3 | 1.7 | <dl | <dl | <dl | 1.7 | 1.9 |
| As | 7.6 | 10.3 | 10.1 | 8.2 | 6.2 | 9.1 | 5.5 | 7.1 | 8.6 | 5.5 | 7.1 | 8.9 | 5.7 | 5.5 | 2.5 | 4.7 |
| Se | <dl | <dl | <dl | <dl | <dl | <dl | <dl | <dl | <dl | <dl | <dl | <dl | 1.1 | 1.0 | 2.4 | <dl |
| Rb | 153 | 75.9 | 90.3 | 60.1 | 13.3 | 42.9 | 266 | 93.6 | 82.9 | 244 | 197 | 46.0 | 10.3 | 10.3 | 175.9 | 263 |
| Sr | 46.8 | 13.6 | 23.9 | 16.3 | 38.3 | 20.4 | 62.5 | 25.4 | 32.2 | 53.5 | 46.9 | 27.5 | 31 | 32 | 53 | 72.2 |
| Y | 22.6 | 8.2 | 14.0 | 9.6 | 7.3 | 7.5 | 28.6 | 11.8 | 11.3 | 25.5 | 17.5 | 8.4 | 7.7 | 7.4 | 19.8 | 23.8 |
| Zr | 67.3 | 17.7 | 36.7 | 26.0 | 9.5 | 14.6 | 129.2 | 32.5 | 36.6 | 117.0 | 61.1 | 21.9 | 9.9 | 13.0 | 78.6 | 83.0 |
| Nb | 10.5 | 3.8 | 6.4 | 4.4 | 1.6 | 2.9 | 20.9 | 6.3 | 5.4 | 19.3 | 11.5 | 4.2 | 1.8 | 1.4 | 11.0 | 14.9 |
| Mo | 0.9 | 1.1 | <dl | <dl | 1.2 | 0.9 | <dl | 1.0 | <dl | <dl | <dl | 1.2 | 1.3 | 1.2 | 0.8 | 0.0 |
| Sn | 3.6 | 1.1 | 1.7 | 1.0 | <dl | 0.8 | 5.1 | 1.8 | 1.9 | 4.9 | 3.3 | 1.2 | 0.9 | 0.8 | 3.6 | 4.6 |
| Sb | 2.4 | <dl | 1.2 | 1.2 | <dl | 4.4 | 0.9 | 1.2 | 1.1 | 0.9 | 1.7 | <dl | 1.1 | <dl | 1.1 | 1.1 |
| Cs | 11.9 | 6.4 | 7.9 | 5.6 | 1.2 | 4.1 | 21.7 | 8.7 | 6.9 | 17.2 | 17.6 | 3.9 | 0.8 | 0.8 | 14.0 | 23.7 |
| Ba | 431 | 183 | 261 | 146 | 45 | 100 | 708 | 227 | 193 | 668 | 443 | 128 | 34.5 | 34.4 | 510.3 | 589 |
| La | 41.6 | 11.6 | 22.8 | 14.2 | 8.6 | 10.6 | 66.4 | 20.3 | 19.7 | 56.2 | 37.7 | 12.7 | 7 | 8 | 32 | 44.0 |
| Ce | 75.0 | 23.0 | 45.3 | 28.5 | 19.4 | 22.7 | 130.6 | 34.7 | 36.0 | 106.3 | 74.8 | 26.6 | 16.0 | 17.0 | 60.3 | 87.4 |
| Pr | 8.6 | 2.5 | 4.5 | 2.9 | 2.0 | 2.4 | 14.1 | 4.3 | 4.0 | 12.0 | 8.1 | 2.8 | 1.7 | 1.9 | 6.9 | 8.9 |
| Nd | 31.4 | 9.8 | 16.9 | 11.1 | 8.1 | 9.3 | 52.7 | 16.4 | 14.9 | 44.5 | 29.9 | 10.5 | 7.0 | 7.4 | 25.0 | 32.4 |
| Sm | 6.9 | 2.3 | 4.1 | 2.7 | 2.0 | 2.4 | 10.7 | 4.1 | 3.1 | 9.8 | 7.0 | 2.6 | 1.6 | 1.6 | 4.5 | 7.4 |
| Eu | 1.3 | <dl | <dl | <dl | <dl | <dl | 1.5 | <dl | <dl | 1.5 | 1.1 | <dl | <dl | <dl | 0.9 | 1.2 |
| Gd | 6.0 | 2.0 | 3.7 | 2.4 | 2.1 | 2.1 | 8.0 | 3.3 | 2.8 | 7.3 | 5.5 | 2.3 | 1.7 | 1.7 | 3.9 | 6.1 |
| Tb | 0.8 | <dl | <dl | <dl | <dl | <dl | <dl | <dl | <dl | 1.0 | <dl | <dl | <dl | <dl | <dl | 0.9 |
| Dy | 4.6 | 1.6 | 2.8 | 1.9 | 1.5 | 1.5 | 5.3 | 2.3 | 2.4 | 5.1 | 3.6 | 1.7 | 1.4 | 1.4 | 3.4 | 4.5 |
| Ho | 0.9 | <dl | <dl | <dl | <dl | <dl | 1.0 | <dl | <dl | <dl | <dl | <dl | <dl | <dl | <dl | <dl |
| Er | 2.3 | 0.9 | 1.6 | 1.1 | <dl | 0.8 | 3.1 | 1.3 | 1.2 | 2.9 | 2.0 | 0.9 | <dl | <dl | 2.0 | 2.6 |
| Yb | 2.2 | 0.9 | 1.5 | 1.0 | <dl | <dl | 3.1 | 1.3 | 1.2 | 2.9 | 1.9 | 0.9 | <dl | <dl | 2.0 | 2.5 |
| Hf | 2.0 | <dl | 1.5 | 1.0 | <dl | <dl | 5.0 | 1.3 | 1.1 | 4.7 | 2.4 | 0.9 | <dl | <dl | 2.1 | 3.6 |
| Ta | 1.2 | <dl | <dl | <dl | <dl | <dl | 1.7 | <dl | <dl | 1.6 | 1.0 | <dl | <dl | <dl | 1.2 | 1.3 |
| W | 2.4 | <dl | 1.1 | 0.8 | <dl | <dl | 3.1 | 1.2 | 1.3 | 2.8 | 1.9 | 0.8 | <dl | <dl | 1.8 | 2.5 |
| Tl | 0.0 | <dl | <dl | <dl | <dl | <dl | 1.2 | <dl | <dl | 1.1 | <dl | <dl | <dl | <dl | 0.7 | 1.0 |
| Pb | 26.4 | 13.8 | 16.1 | 19.9 | 15.0 | 8.8 | 5.2 | 12.9 | 14.6 | 7.9 | 13.3 | 14.4 | 44.9 | 9.8 | 13.4 | 27.3 |
| Bi | <dl | <dl | <dl | <dl | <dl | <dl | <dl | <dl | <dl | <dl | <dl | <dl | <dl | <dl | <dl | <dl |
| Th | 16.2 | 7.2 | 11.9 | 8.0 | 4.7 | 5.9 | 26.1 | 9.0 | 9.2 | 24.0 | 16.6 | 5.8 | 4.6 | 4.5 | 12.3 | 18.5 |
| U | 3.5 | 1.6 | 2.5 | 1.8 | 1.0 | 1.3 | 5.5 | 2.1 | 2.1 | 5.1 | 3.5 | 1.8 | <dl | <dl | 2.5 | 4.5 |

*Contents of Al, Si, Ca, Fe, K, Mg, Na, S, and P are in %, and those of remaining trace elements are in mg/kg. < dl, below detection limit; a: average of Worldwide coals from Ketris and Yudovich (2009).

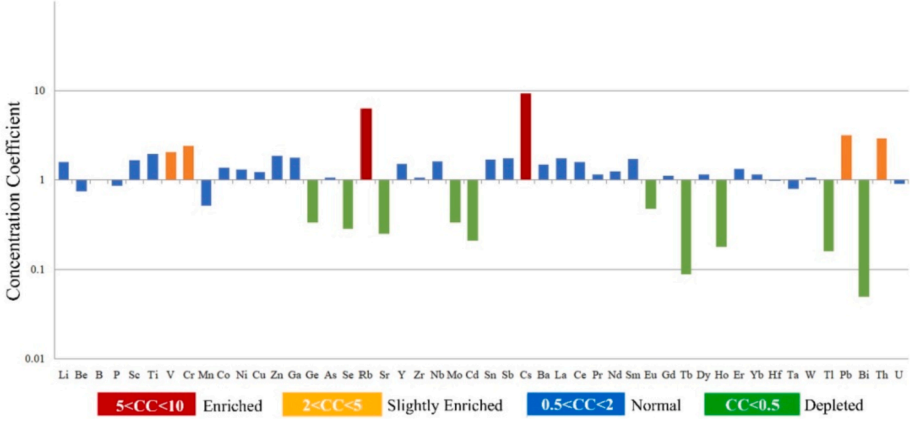


**Fig. 8.** Concentration coefficient (CC) of coals and parting clays in Coc Sau mine, Cam Pha coalfield compared to world hard coals. Data of world hard coals is from Ketris and Yudovich (2009).

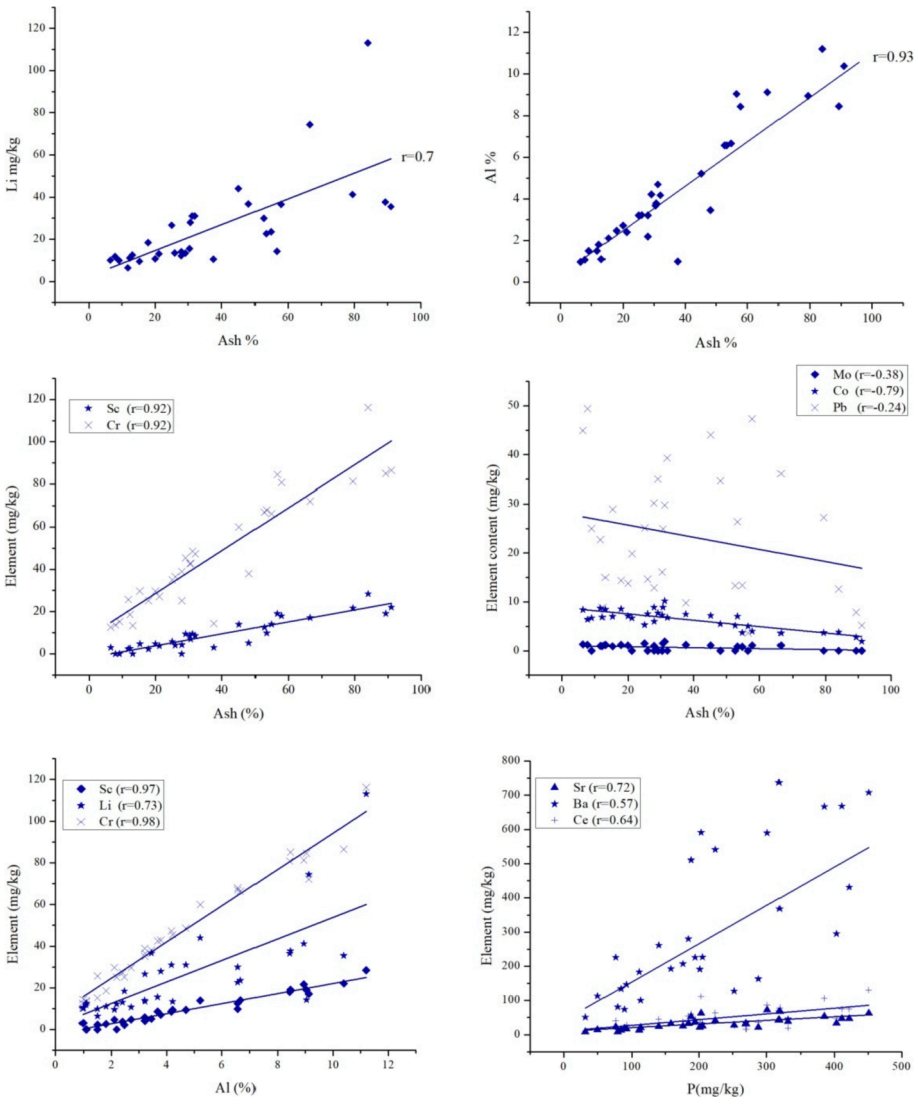


**Fig. 9.** Correlation of Al, P and ash yields with some selected trace elements in Coc Sau coal.

deposited under fresh water-influenced environments, which is also consistent with previous studies on coal-forming environments in this area (Hien and Binh, 1966a,b; Hung and Huu, 1996; Tien, 1969; Tri et al., 1977). Consequently, the mineral matters and trace elements in coals were to a large extent influenced by the terrigenous input as discussed below.

### 5.2. Sedimentary source rocks

The $Al_2O_3/TiO_2$ ratio is commonly used to indicate an initial sediment source of clastic sedimentary rocks (Hayashi et al., 1997), and coal seams (Dai et al., 2015a,b,c, 2017b, 2017c). The variation of $Al_2O_3/TiO_2$ ratio of 3–8, 8–21, 21–70 respectively represents mafic, intermediate, and felsic rocks (Hayashi et al., 1997). With the exception in sample Day-7 (19.2) and Day-33 (19.1), the $Al_2O_3/TiO_2$ ratio of the other coal and host samples varies from 21.3 to 42.6 (Fig. 11), inferring that sediment provenance of the peat swamp was mostly of felsic rocks.

In addition, L-type REY enrichment pattern in coal bearing sequences is indicative of a terrigenous origin (Dai et al., 2016). As aforementioned, most of the coal and host rock samples in the Coc Sau mine are characterized by L-type REY enrichment patterns, which is consequently inherited from the felsic sediment-source region. Furthermore, weak negative Ce and distinct negative Eu anomalies are indicative of felsic or felsic-intermediate source origins (Dai et al., 2016). The Coc Sau coals mostly display negative Eu and weak or no negative Ce anomalies, which further indicate that the terrigenous inputs of coal-forming peat swamp were derived from felsic sediments source region, which is further evidenced by the felsic sediment source rocks of the Paleozoic and Mesozoic dominantly from the north of the Hon Gai graben, which is mainly composed of sandstone, siltstone, tuffaceous sandstone, interbeds of gritstone, sericite schist, quartz-schist and siltstone of the Tẳn Mài formation (Ordovician-Silurian) and the porphyritic rhyolite and dacite, conglomerate, tuffaceous sandstone, tuffaceous siltstone, felsite and rhyolite of the Binh Lieu formation (Middle Triassic, Anisian) (Luong, 1970; Sao, 1973; Tien; 1969).

### 5.3. Enrichment of Rb and Cs in the Coc Sau coals

Seredin (2003) has found that Rb and Cs presents significant economic value in the Spetzugli Ge-bearing brown coal, which could be

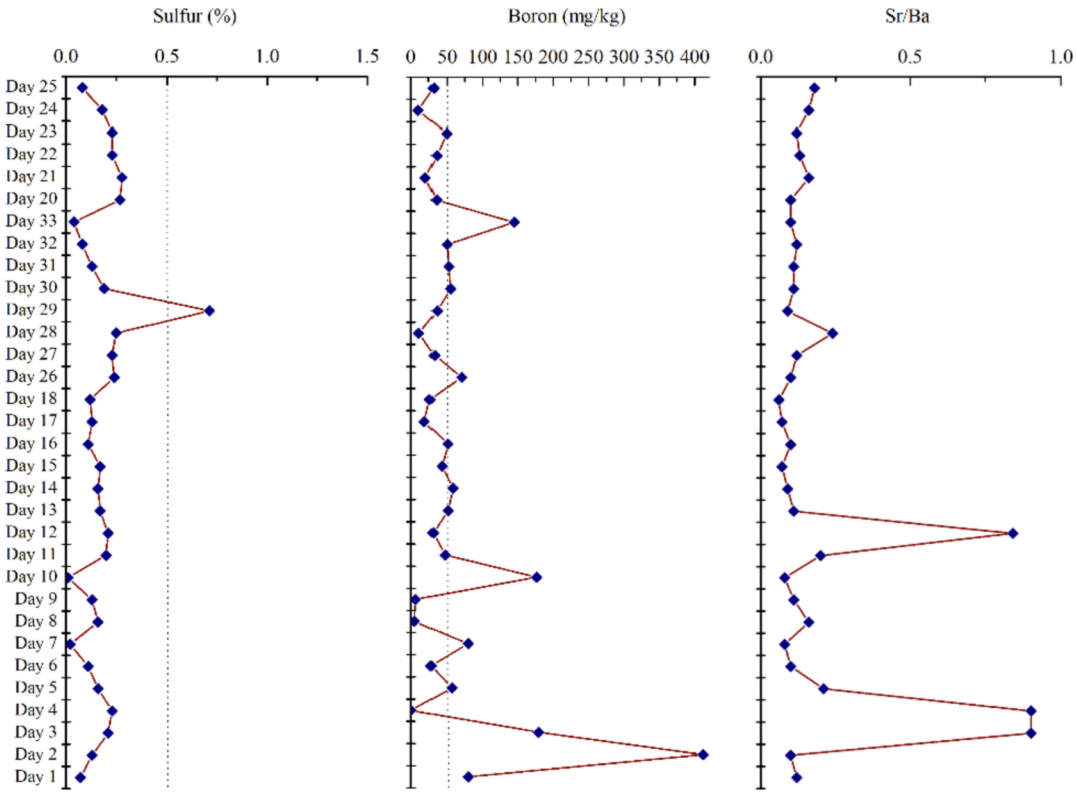


**Fig. 10.** Vertical distribution of elements in late Triassic coal seam. A: Sulphur; B: Boron.

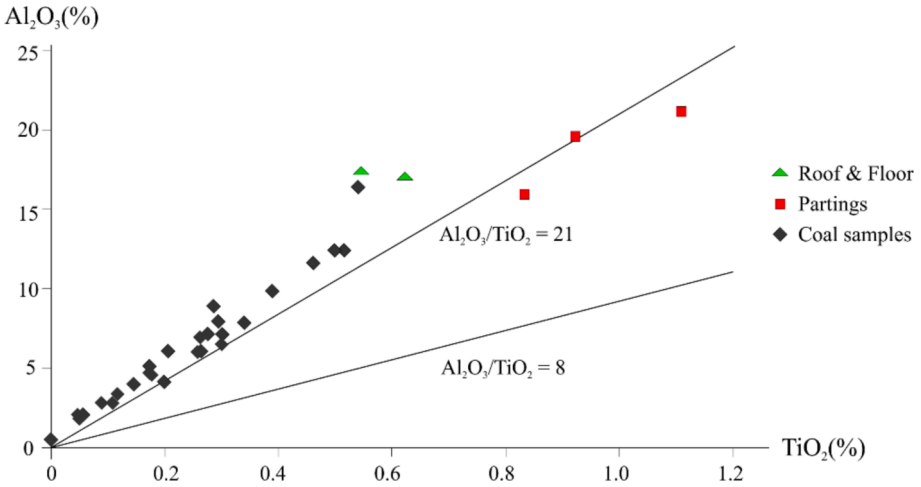


**Fig. 11.** $Al_2O_3$ versus $TiO_2$ in coals and non-coal rocks in Coc Sau surface mine, Cam Pha coalfiled.

exploited as a byproduct. As mentioned above, Rb and Cs are highly enriched in the Coc Sau coals. The average content of Rb is 89.2 mg/kg in coals, and 239 mg/kg in non-coal rocks (roof/floor/parting), while the average content of Cs is 9.4 mg/kg in coals and 32.3 mg/kg in non-coal rocks, much higher than those in world hard coals reported by Ketris and Yudovich (2009). The elevated Rb and Cs in coal can be a potential source for Rb and Cs recovery from the studied coals during coal utilization and combustion.

Ward et al. (1999) reported that Rb is remarkably correlated with K in Permian coals. Fig. 12 illustrates the vertical variation of Rb, Al, K, and ash yield in the studied coal samples, and it is obvious that Rb has a similar distribution trend with Al, K, and ash yield. In addition, Rb concentration is also positively correlated to Al ($r = 0.97$) and K ($r = 0.98$) content as well as ash yield ($r = 0.92$, Fig. 13), pointing to an inorganic affinity of Rb. In addition, the correlation coefficient of Rb with K is higher than that with Al, indicating Rb is closely associated with K and most likely occurs in K-rich clay minerals (e.g., muscovite and to a lesser extent illite) in the present study.

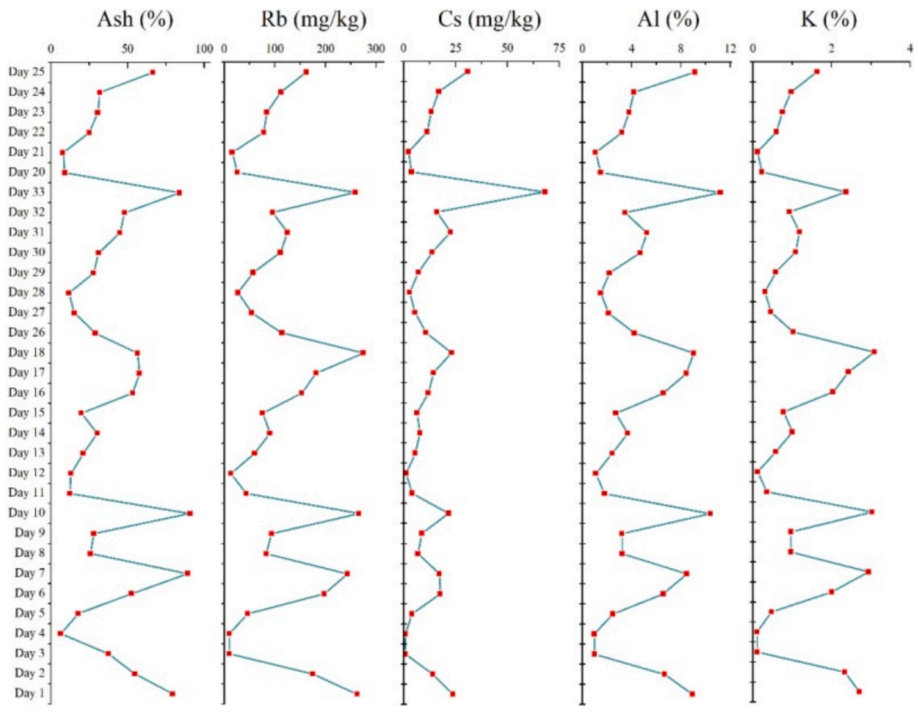


**Fig. 12.** Vertical variation of Ash, Rb, Cs, Al and Potassium in Coc Sau coal.

With respect to cesium, it probably occurs in K-bearing clay minerals (e.g., illite and smectite), or is adsorbed by organic matter in coal (Swaine, 1990). In the present research, cesium not only has the similar vertical variation with Al, K, and ash yield (Fig. 12), but also is obviously correlated with Al ($r = 0.82$), K ($r = 0.64$), ash yield ($r = 0.73$, Fig. 13), indicating that Cs is predominantly associated with inorganic minerals, especially K-rich clay minerals (e.g., muscovite in the studied coals), which are the main carriers of Cs. Because rubidium has the same molecular radius as potassium and cesium has a larger molecular radius than potassium, thus the correlation coefficient between Rb and K is much higher than the correlation between Cs and K (Fig. 13).

Previous studies have also shown that Rb and Cs largely occurs in illite and mixed-layer clays substituting for K in these minerals (Seredin, 2003; Zhao et al., 2017; Finkelman et al., 2018). Therefore, all of the results discussed above indicate that K-rich clay minerals, such as muscovite and to a lesser extent illite, are the major carrier of both Rb and Cs enrichment in the late Triassic GII coals from the Coc Sau mine.

With respect to the origin of the elevated Rb and Cs, Seredin (2003) ascribed the anomalous enrichment of Rb in the Spetsugli Germanium deposits to its high content in volcanogenic Ge-bearing solutions circulating in rocks of the coal-bearing molasse. Xiao et al. (2018) attributed the enrichment of W, Rb, and Cs in Late Permian Meitian coals in Southern China to magmatic hydrothermal activity. As aforementioned, the enrichment of Rb and Cs in the current study occurs not only in coal but also in non-coal rock, indicating that sedimentary source rocks of the Coc Sau coal mine during the late Triassic period are potential source of anomalous Rb and Cs. The terrigenous source sediments of Hon Gai graben are most likely derived from the parent felsic rocks from surrounding regions which is rich in feldspar and mica and transported into the coal basin by the weathering process during the sedimentation stage.

## 6. Conclusion

The late Triassic coals from the Coc Sau surface mine, Cam Pha coalfiled, Quang Ninh coal basin, Vietnam are characterized by low moisture and sulfur content, high ash yield, and low volatile matter content, pointing to semianthracite rank. Minerals occurring in the Coc Sau coals are predominantly composed of quartz, kaolinite, muscovite, with minor proportions of anatase, ankerite and calcite, and trace amount of clinochlore. With the exception of the carbonate minerals, eg. calcite and ankerite in the Coc Sau coals that were primarily formed during epigenesis, most of the other mineral phases in the studied coals are dominantly of authigenic origin, and originated from the terrigenous sediments.

In comparison to worldwide hard coals, the late Triassic Coc Sau coals are enriched in Rb and Cs, and to a lesser extent, V, Cr, Pb, and Th. The elevated Rb and Cs largely occurs in clay minerals, especially K-rich clay minerals, such as muscovite in the Coc Sau coals.

The late Triassic Coc Sau coals are deposited in a limnic environment with high terrigenous input, as indicated by low sulfur content and Sr/Ba, high ash yields and high abundance of kaolinite in the coals. The elevated Rb and Cs in the Coc Sau coals are also originated from the terrigenous source region surrounding the basin, and can be a potential source for Rb and Cs recovery from the Coc Sau coals.

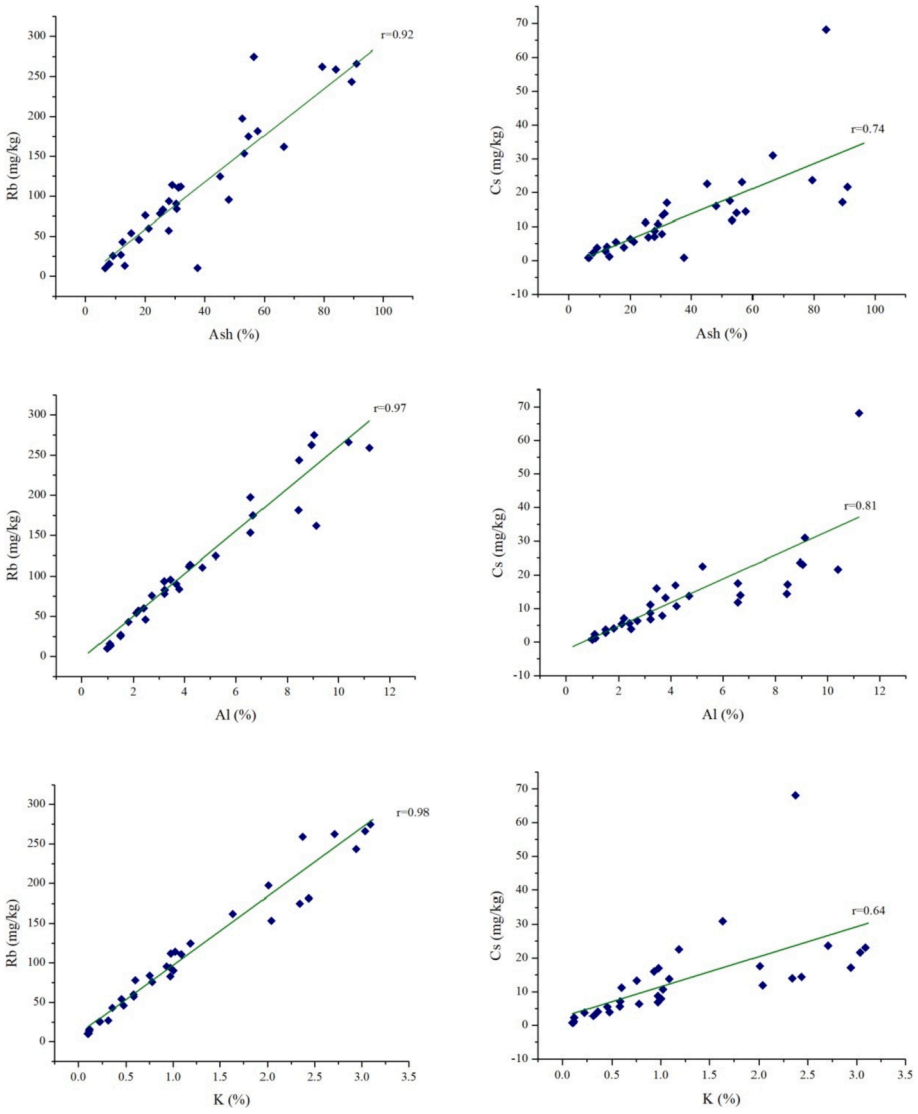


**Fig. 13.** Correlation coefficient between Rb and Cs with ash and selected major elements in bench coal.

## Author Contributions

All authors have read and agreed to the published version of the manuscript.

## Funding

This research was supported by the National Nature Science Foundation of China (Nos. 41972179, 41972180), the National Key R&D Program of China (No. 2021YFC29022005), the Fundamental Research Funds for the Central Universities, China University of Geosciences (Wuhan) (No. CUGCJ1819), and the Key Project of Coal-based Low-carbon Joint Research Foundation of NSFC and Shanxi Province (No. U1910204). The authors would like to acknowledge Coc Sau coal join stock company for assistance in sampling and acknowledge Institute of Environmental Assessment and Water Research, CSIC, Spain for assistance with the sample analysis.

## Declaration of Competing Interest

The authors declare that they have no known competing financial interests or personal relationships that could have appeared to influence the work reported in this paper.

## Acknowledgments

The authors appreciate the reviewers for their useful comments and suggestions to improve the quality of the manuscript.

## References

ASTM D388-12, 2012. Standard Classification of Coals by Rank. ASTM International, West Conshohocken, PA.
ASTM Standard D3173-11, 2011. Test Method for Moisture in the Analysis Sample of Coal and Coke. ASTM International, West Conshohocken, PA, USA.
ASTM Standard D3174-11, 2011. Annual Book of ASTM Standards. In Test Method for Ash in the Analysis Sample of Coal and Coke; ASTM International: West Conshohocken, PA, USA.
ASTM Standard D3175-11, 2011. Test Method for Volatile Matter in the Analysis Sample of Coal and Coke. ASTM International, West Conshohocken, PA, USA.
Banerjee, I., Goodarzi, F., 1990. Paleoenvironment and sulfur-boron contents of the Mannville (Lower Cretaceous) coals of southern Alberta, Canada. Sed. Geol. 67 (3-4), 297–310.
Baruya, P., 2010. Prospects for Coal and Clean Coal Technologies in Vietnam. IEA Clean Coal Centre, CCC/164, ISBN 978-929029-484-9, February 2010. http://www.iea-coal.org.uk/documents/82299/7465/Prospects-for-coaland-clean-coal-technologies-in-Vietnam-(CCC/164).
Binh, N., 2005. On the Indosinian tectonic cycle in North Vietnam. J. Geol. 291, 11–12.
Boudou, G.P., Schimmelmann, A., Ader, M., et al., 2008. Organic nitrogen chemistry during low-grade metamorphism. Geochim. Cosmochim. Acta 72.

Brownfield, M.E., Affolter, R.H., Stricker, G.D., Hildebrand, R.T., 1995. High chromium contents in Tertiary coal deposits of northwestern Washington - A key to their depositional history. Int. J. Coal Geol. 27 (2-4), 153–169.
Chen, J., Chen, P., Yao, D., Liu, Z., Wu, Y., Liu, W., Hu, Y., 2015. Mineralogy and geochemistry of Late Permian coals from the Donglin Coal Mine in the Nantong coalfield in Chongqing, southwestern China. Int. J. Coal Geol. 149, 24–40.
Chinh, L.D., Gheewala, S.H., Bonnet, S., 2007. Integrated environmental assessment and pollution preventionin Vietnam: the case of anthracite production. J. Cleaner Prod. 15 (18), 1768–1777.
Chung, F.H., 1974. Quantitative interpretation of X-ray diffraction patterns of mixtures: I. Matrix flushing method for quantitative multicomponent analysis. J. Appl. Crystalogr. 7 (6), 519–525.
Dai, S., Bechtel, A., Eble, C.F., Flores, R.M., French, D., Graham, I.T., Hood, M.M., Hower, J.C., Korasidis, V.A., Moore, T.A., Püttmann, W., Wei, Q., Zhao, L., O'Keefe, J.M.K., 2020. Recognition of peat depositional environments in coal: A review. Int. J. Coal Geol. 219, 103383.
Dai, S., Finkelman, R.B., 2018. Coal as a promising source of critical elements: Progress and future prospects. Int. J. Coal Geol. 186, 155–164.
Dai, S., Finkelman, R.B., French, D., Hower, J.C., Graham, I.T., Zhao, F., 2021. Modes of occurrence of elements in coal: A critical evaluation. Earth-Sci. Rev. 222, 103815.
Dai, S., Graham, I.T., Ward, C.R., et al., 2016. A review of anomalous rare earth elements and yttrium in coal. Int. J. Coal Geol. 159.
Dai, S., Li, T., Jiang, Y., Ward, C.R., Hower, J.C., Sun, J., Liu, J., Song, H., Wei, J., Li, Q., Xie, P., Huang, Q., 2015c. Mineralogical and geochemical compositions of the Pennsylvanian coal in the Hailiushu Mine, Daqingshan Coalfield, Inner Mongolia, China: Implications of sediment-source region and acid hydrothermal solutions. Int. J. Coal Geol. 137, 92–110.
Dai, S., Ren, D., Chou, C.-L., Finkelman, R.B., Seredin, V.V., Zhou, Y., 2012. Geochemistry of trace elements in Chinese coals: A review of abundances, genetic types, impacts on human health, and industrial utilization. Int. J. Coal Geol. 94, 3–21.
Dai, S., Seredin, V.V., Ward, C.R., Hower, J.C., Xing, Y., Zhang, W., Song, W., Wang, P., 2015a. Enrichment of U-Se–Mo–Re–V in coals preserved within marine carbonate successions: geochemical and mineralogical data from the Late Permian Guiding Coalfield, Guizhou. China. Int. J. Coal Geol. 50 (2), 159–186.
Dai, S., Seredin, V.V., Ward, C.R., Jiang, J., Hower, J.C., Song, X., Jiang, Y., Wang, X., Gornostaeva, T., Li, X., Liu, H., Zhao, L., Zhao, C., 2014. Composition and modes of occurrence of minerals and elements in coal combustion products derived from high-Ge coals. Int. J. Coal Geol. 121, 79–97.
Dai, S., Ward, C.R., Graham, I.T., French, D., Hower, J.C., Zhao, L., Wang, X., 2017a. Altered volcanic ashes in coal and coal-bearing sequences: A review of their nature and significance. Earth Sci. Rev. 175, 44–74.
Dai, S., Xie, P., Jia, S., Ward, C.R., Hower, J.C., Yan, X., French, D., 2017b. Enrichment of U-Re-V-Cr-Se and rare earth elements in the Late Permian coals of the Moxinpo Coalfield, Chongqing, China: Genetic implications from geochemical and mineralogical data. Ore Geol. Rev. 80, 1–17.
Dai, S., Xie, P., Ward, C.R., Yan, X., Guo, W., French, D., Graham, I.T., 2017c. Anomalies of rare metals in Lopingian super-high-organic-sulfur coals from the Yishan Coalfield, Guangxi. China. Ore Geol. Rev. 88, 235–250.
Dai, S., Yan, X., Ward, C.R., Hower, J.C., Zhao, L., Wang, X., Zhao, L., Ren, D., Finkelman, R.B., 2018. Valuable elements in Chinese coals: a review. Int. Geol. Rev. 60 (5-6), 590–620.
Dai, S., Yang, J., Ward, C.R., Hower, J.C., Liu, H., Garrison, T.M., French, D., O'Keefe, J. M.K., 2015b. Geochemical and mineralogical evidence for a coal-hosted uraniumdeposit in the Yili Basin, Xinjiang, northwestern China. Ore Geol. Rev. 70, 1–30.
Dai, S., Zhang, W., Seredin, V.V., Ward, C.R., Hower, J.C., Song, W., Wang, X., Li, X., Zhao, L., Kang, H., Zheng, L., Wang, P., Zhou, D., 2013a. Factors controlling geochemical and mineralogical compositions of coals preserved within marine carbonate successions: A case study from the Heshan Coalfield, southern China. Int. J. Coal Geol. 2013 (109–110), 77–100.
Dai, S., Zhang, W., Ward, C.R., Seredin, V.V., Hower, J.C., Li, X., Song, W., Wang, X., Kang, H., Zheng, L., Wang, P., Zhou, D., 2013b. Mineralogical and geochemical anomalies of late Permian coals from the Fusui Coalfield, Guangxi Province, southern China: Influences of terrigenous materials and hydrothermal fluids. Int. J. Coal Geol. 105, 60–84.
Finkelman, R.B., Tian, L., 2017. The health impacts of coal use in China. Int. Geol. Rev. 60 (5-6), 579–589.
Finkelman, R.B., Dai, S., French, D., 2019. The importance of minerals in coal as the hosts of chemical elements: A review. Int. J. Coal Geol. 212, 103251.
Finkelman, R.B., Orem, W., Castranova, V., Tatu, C.A., Belkin, H.E., Zheng, B., Lerch, H. E., Maharaj, S.V., Bates, A.L., 2002. Health impacts of coal and coal use: possible solutions. Int. J. Coal Geol. 50 (1-4), 425–443.
Finkelman, R.B., Palmer, C.A., Wang, P., 2018. Quantification of the modes of occurrence of 42 elements in coal. Int. J. Coal Geol. 185, 138–160.
Goodarzi, F., Gentzis, T., 1987. Depositional Setting, Determined by Organic Petrography, of the Middle Eocene Hat Creek No. 2 Coal Deposit, British Columbia, Canada. Bull. Can. Petrol. Geol. 35, 197–211.
Goodarzi, F., Swaine, D.J., 1994. Paleoenvironmental and environmental implications of the boron content of coals. Geological Survey of Canada Bulletin 471.
Hayashi, K.-I., Fujisawa, H., Holland, H.D., Ohmoto, H., 1997. Geochemistry of ~1.9 Ga sedimentary rocks from northeastern Labrador, Canada. Geochim. Cosmochim. Acta 61 (19), 4115–4137.
Hien, P.T., Binh, V., 1966a. Characteristics of lithological facies of coal-bearing sediments in the Cam Pha and practical conclusions. J. Geol. 57, 15–24.
Hien, P.T., Binh, V.Q., 1966b. Sequence of coal-bearing sediments in the Cam Pha. J. Geol. 60, 14–20.
Hoang, N.K., Dang, T.Q., Hoang, T.D., Le, D.K., Nguyen, Q.M., Nguyen, T.C., 2001. Geology and Mineral Resources of Hai Phong Sheet. Explanatory Note to Geological Map of Vietnam. Department of Geology and Minerals of Vietnam, Hanoi.
Hower, J.C., Dai, S., Eskenazy, G., 2016. Distribution of uranium and other radionuclidesin coal and coal combustion products, with discussion of occurrences of combustion products in Kentucky Power Plants. Coal Combust. Gasif. Prod. 8, 44–53.
Hung, L., 1997. Geology and Mineral Resources Mapping of Cam Pha in 1:50,000 Scale. Vietnam Institute of Geosciences and Mineral Resources, Hanoi, Vietnam.
Hung, L., Huu, N.D., 1996. New data on geology and mineral resources of Cam Pha-Ba Che Region. J. Geol. 5, 141–157.
Ich, T., Chi, N.T., 1972. Cause and law of metamorphism of coal in Quang Ninh and the Ha Noi depression. J. Geol. 103, 16–19.
Karayigit, A.I., Bircan, C., Oskay, R.G., Türkmen, İ., Querol, X., 2020. The geology, mineralogy, petrography, and geochemistry of the MioceneDursunbey coal within fluvio-lacustrine deposits, Balıkesir (Western Turkey). Int. J. Coal Geol. 228, 103548.
Ketris, M.P., Yudovich, Y.E., 2009. Estimations of Clarkes for Carbonaceous biolithes: World averages for trace element contents in black shales and coals. Int. J. Coal Geol. 78 (2), 135–148.
Li, J., Zhuang, X., Querol, X., et al., 2012. High quality of Jurassic coals in the southern and eastern Junggar coalfields, Xinjiang, NW China: geochemical and mineralogical characteristics. Int. J. Coal Geol. 99.
Luong, T., 1970. Indosinid structure in North Vietnam and its tectonic development history. J. Geol. 91–92, 46–57.
Permana, A.K., Ward, C.R., Li, Z., et al., 2013. Distribution and origin of minerals in high-rank coals of the South Walker Creek area, Bowen Basin, Australia. Int. J. Coal Geol. 116-117.
Quang, P., 1969. Age of Hong Gai coal-bearing sediments in and problems of regional geology in Mesozoic. J. Geol. 87–88, 13–39.
Quang, P., 1971. Tectonics of the coal basin in Northeast Bac Bo. J. Geol. 97, 1–15.
Querol, X., Izquierdo, M., Monfort, E., Alvarez, E., Font, O., Moreno, T., Alastuey, A., Zhuang, X., Lu, W., Wang, Y., 2008. Environmental characterization of burnt coal gangue banks at Yangquan, Shanxi Province, China. Int. J. Coal Geol. 75 (2), 93–104.
Querol, X., Whateley, M.K.G., Fernández-Turiel, J.L., Tuncali, E., 1997. Geological controls on the mineralogy and geochemistry of the Beypazari lignite, central Anatolia, Turkey. Int. J. Coal Geol. 33 (3), 255–271.
Sao, H., 1973. Coal forming stages in North Viet Nam. J. Geol. 109, 16–25.
Seredin, V.V., Dai, S., 2012. Coal deposits as potential alternative sources for lanthanides and yttrium. Int. J. Coal Geol. 94, 67–93.
Seredin, V.V., Finkelman, R.B., 2008. Metalliferous coals: A review of the main genetic and geochemical types. Int. J. Coal Geol. 76 (4), 253–289.
Seredin, V., 2003. Anomalous concentrations of trace elements in the Spetsugli Germanium deposits (Pavlovka Brown Coal Deposit, Southern Primorye): communication 2. Rubidium and Cesium. Lithol. Miner. Resour. 38, 233–241.
Swaine, D., Goodarzi, F., 1995. Environmental Aspects of Trace Elements in Coal. Springer, Netherlands, p. 312.
Spiro, B.F., Liu, J., Dai, S., et al., 2019. Marine derived $^{87}Sr/^{86}Sr$ in coal, a new key to geochronology and palaeoenvironment: Elucidation of the India-Eurasia and China-Indochina collisions in Yunnan, China. Int. J. Coal Geol. 215.
Swaine, D.J., 1990. Trace Elements in Coal. Butterworths, London, p. 294.
Tien, P., 1969. On the stratigraphy, lithofacies and forming conditions of the Hon Gai - Cam Pha coal band. J. Geol. 83–84, 15–28.
Tieu, P., 1971. The Red River tectonic wedge and formation of fuel resources. J. Geol. 95, 28–30.
Tri, T., et al., 1977. Geology of Vietnam: The North Part. Publishing House for Science and Technology, p. 354 in Vietnamese.
Tri, T., et al., 2000. Mineral Resources of Vietnam. Department of geology and minerals of Vietnam, Vietnam, Hanoi, p. 214.
Tri, T., Khuc, V., 2011. Geology and Earth Resources of Vietnam. Publishing House for Science and Technology, p. 634.
Ward, C.R., Spears, D.A., Booth, C.A., Staton, I., Gurba, L.W., 1999. Mineral matter and trace elements in coals of the Gunnedah Basin, New South Wales, Australia. Int. J. Coal Geol. 40 (4), 281–308.
Ward, C.R., 2002. Analysis and significance of mineral matter in coal seams. Int. J. Coal Geol. 50 (1-4), 135–168.
Xiao, Z., Cao, Y., Jiang, W., Zhou, P., Huang, Y., Liu, J., 2018. Minerals and Enrichment of W, Rb, and Cs in Late Permian Coal from Meitian Mine, Meitian Coalfield, Southern China by Magmatic Hydrothermal Fluids. Minerals 8 (11), 504.
Yan, X., Dai, S., Graham, I.T., French, D., Hower, J.C., 2019. Mineralogy and geochemistry of the Palaeogene low-rank coal from the Baise Coalfield, Guangxi Province, China. Int. J. Coal Geol. 214, 103282.
Yang, N., Tang, S., Zhang, S., Chen, Y., 2016. Modes of occurrence and abundance of trace elements in Pennsylvanian coals from the Pingshuo Mine, Ningwu Coalfield, Shanxi Province, China. Minerals 6 (2), 40.
Zhao, C., Liu, B., Xiao, L., Li, Y., Liu, S., Li, Z., Zhao, B., Ma, J., Chu, G., Gao, P., Sun, Y., 2017. Significant enrichment of Ga, Rb, Cs, REEs and Y in the Jurassic No. 6 coal in the Iqe Coalfield, northern Qaidam Basin, China - A hidden gem. Ore Geol. Rev. 83, 1–13.